UNIVERSITY OF HELSINKI REPORT SERIES IN PHYSICS

HU-P-D219

INELASTIC X-RAY SCATTERING PERSPECTIVE ON AQUEOUS SOLUTIONS

Iina Juurinen

Division of Materials Physics
Department of Physics
Faculty of Science
University of Helsinki
Helsinki, Finland

ACADEMIC DISSERTATION

To be presented, with the permission of the Faculty of Science of the University of Helsinki, for public examination in auditorium LS1, Chemicum, A. I. Virtasen aukio 1, on 17th of October 2014 at 12:15.

Helsinki 2014

Supervisors

Prof. Keijo Hämäläinen
Department of Physics
University of Helsinki
Helsinki, Finland

Dr. Mikko Hakala
Department of Physics
University of Helsinki
Helsinki, Finland

Pre-examiners

Prof. Juha Vaara
University of Oulu
Oulu, Finland

Dr. Christian Sternemann
Technische Universität Dortmund
Dortmund, Germany

Opponent

Prof. John Tse
University of Saskatchewan
Saskatoon, Canada

Custos

Prof. Keijo Hämäläinen
Department of Physics
University of Helsinki
Helsinki, Finland

Report Series in Physics HU-P-D219
ISSN 0356-0961

ISBN 978-952-10-8963-3 (printed version)
Picaset Oy
Helsinki 2014

ISBN 978-952-10-8964-0 (pdf version)
http://ethesis.helsinki.fi/
Helsingin Yliopiston verkkojulkaisut
Helsinki 2014

Preface

The research for this thesis was carried out at the Department of Physics of the University of Helsinki. I am thankful to the head of the department, Prof. Hannu Koskinen, for the opportunity to work at the Department of Physics. I thank the National Graduate School in Materials Physics (NGSMP) and the Academy of Finland for providing the financial support for this thesis.

Science is all about collaborating and working together. Thus, I have many people to thank. First of all, I thank my supervisor, Prof. Keijo Hämäläinen, for being enthusiastic and inspiring head of the group, the faculty, and also the university. Also, I like to thank my more hands-on supervisor, Dr. Mikko Hakala, for all of the help and advice during these years. Additionally, Dr. Simo Huotari, my unofficial third supervisor, has been important especially to the experimental side of the work, and I am grateful for his guidance.

I think it is fair to say that I would have not accomplished this thesis without help, advice, and encouragement from Dr. Tuomas Pylkkänen. I am truly grateful for all the things Tuomas has taught me, which is nearly everything I know about x-ray physics and liquids (and photography, computers, phones, wines, movies, how to survive in France, and so forth...), and the patience he has had teaching all the aforementioned things to me.

It has been a pleasure to work with the whole "Helixs" group. Especially, I thank Dr. Christoph Sahle, for his advice, ideas, encouragement, and super speedy replies to the "Dear co-authors, ..." messages, and Dr. Szabolcs Galambosi, Dr. Arto Sakko, Dr. Johannes Niskanen, Dr. Susi Lehtola, Kari Ruotsalainen and Jaakko Koskelo for their support and all their help with everything that has come by. Jaakko, my office mate for the past couple of years, deserves extra credit for being so patient with my frequent random outbursts, answering to my various more-or-less stupid questions, and helping me to come up with titles for things. I thank all my co-authors for the work they have done, and I acknowledge the European Synchrotron Radiation Facility (ESRF) and it's highly professional staff for enabling us to carry out the demanding experimental work.

It has been a great experience to work at the x-ray laboratory, and, obviously, it is the people there that makes it enjoyable. I wholeheartedly thank my colleagues for making the work days brighter. Especially, I thank the x-ray floorball team for giving us – those less inclined to hurt themselves – a nice quiet hour of work every week.

I have the privilege of having friends all over the world. The support, understanding, and caring that carries even from across the seas is astonishing. I thank all my friends

for all the fun, seriousness, and everything in between, and for being crazy enough to keep me sane.

Finally, I thank my family. My parents and brother are amazing, and I am grateful for their care and support, and for encouraging me to become who I am. Additionally, I thank Tessa for showing how life should be enjoyed. Above all, I thank Tuomas – for love and everything that comes with it.

I. Juurinen: Inelastic x-ray scattering perspective on aqueous solutions, University of Helsinki, 2014, 48 pages + appendices. University of Helsinki, Report Series in Physics HU-P-D219.

Keywords: hydrogen bonding, aqueous mixtures, liquids, water, inelastic x-ray scattering, x-ray Raman scattering, Compton scattering

Abstract

Not only being essential to life as we know it water also has peculiar behaviour in comparison to other liquids. The macroscopic anomalies of water are driven by its microscopic structure. It is agreed upon that the molecular-level structure of liquid water is highly structured due to its extensive hydrogen-bond network. However, the details on the structure remain debated. Moreover, it is surprising how little is known about the behaviour of water when it interacts with other substances, taken how important water is as a solvent.

Studying the structure of liquids is not straightforward and each method has its particular sensitivity. Inelastic x-ray scattering is a versatile method for structural analyses, and thus can provide information from a new perspective. Compared to many other techniques it has several advantages when investigating liquids: for example, bulk structures can be studied and no vacuum environment is needed. In the element-sensitive x-ray Raman scattering the electronic excitations from core to unoccupied molecular orbitals reveal the local environment. On the other hand, information on the electronic structure is also obtained with x-ray Compton scattering, in which the ground-state electron momentum distribution is probed.

In this thesis, the problematics of the hydrogen-bond network of water is approached by observing the effects other components have on it with x-ray Raman and Compton scattering. The thesis includes studies on ionic, hydrophobic, and hydrophilic interaction, particularly in aqueous LiCl, water-alcohol mixtures and aqueous polymer poly(N-isopropylacrylamide). The information obtained from these systems both elucidates the structure of the hydrogen-bond network of water, and further affirms the benefit of inelastic x-ray scattering methods in studying a wide range of disordered materials.

List of papers

This thesis consists of an introductory part and four research articles, which are referred to by the Roman numerals **I**–**IV** throughout the text.

I **I. Juurinen**, T. Pylkkänen, K. O. Ruotsalainen, Ch. J. Sahle, G. Monaco, K. Hämäläinen, S. Huotari and M. Hakala. *Saturation Behavior in X-ray Raman Scattering Spectra of Aqueous LiCl*, The Journal of Physical Chemistry B, **117**, 16506 (2013).

II **I. Juurinen**, T. Pylkkänen, Ch. J. Sahle, L. Simonelli, K. Hämäläinen, S. Huotari and M. Hakala. *Effect of the Hydrophobic Alcohol Chain Length on the Hydrogen-Bond Network of Water*, The Journal of Physical Chemistry B, **118**, 8750 (2014).

III **I. Juurinen**, K. Nakahara, N. Ando, T. Nishiumi, H. Seta, N. Yoshida, T. Morinaga, M. Itou, T. Ninomiya, Y. Sakurai, E. Salonen, K. Nordlund, K. Hämäläinen, and M. Hakala. *Measurement of Two Solvation Regimes in Water-Ethanol Mixtures Using X-Ray Compton Scattering*, Physical Review Letters, **107**, 197401 (2011).

IV **I. Juurinen**, S. Galambosi, A. G. Anghelescu-Hakala, J. Koskelo, V. Honkimäki, K. Hämäläinen, S. Huotari and M. Hakala. *Molecular-Level Changes of Aqueous Poly(N-isopropylacrylamide) in Phase Transition*, The Journal of Physical Chemistry B, **118**, 5518 (2014).

The papers **I**–**IV** are included as appendices in the printed version of this thesis and they have been reprinted with kind permission from the publishers.

Author's contribution

The author of this thesis planned the experiment in paper **II**, participated in the experiments in papers **I**, **II**, and **IV**, analysed the experimental results in paper **IV**, planned and performed the computational work in all papers, interpreted the results in all papers, and wrote papers **I**, **II**, and **IV**, and was actively involved in writing of paper **III**.

Contents

1 Introduction

Water's role as the solvent of life makes it ever so interesting. Water covers more than 70% of the Earth surface and it is essential for our survival on Earth - not just as something to drink or clean with, but vital to the biological processes in our bodies. For example, water is a key player in protein folding, [1, 2] or creating the cell membrane surface, [3] and DNA would not have the double-helix structure if it would not be solvated in water.

Given the importance of water, it is surprising how little is actually known about it. We know that a water molecule consists of three atoms: one oxygen and two hydrogens. Due to their polarity, water molecules can form hydrogen bonds with other water molecules. Hydrogen bonding makes water a quite unique substance. There are over seventy anomalous properties of water, and most likely not all of them are even discovered yet. For example, water in solid form (ice) is less dense than liquid water, and additionally, the density of liquid water is not a linear function of temperature as water is most dense at 4 °C.

Although the existence of a hydrogen-bond network in water is generally agreed upon, the details of the microscopic structure of water have been under heated debate for a long time. Since 1933, the general idea of the hydrogen-bond network of liquid water has been that it is on average a tetrahedrally arranged fluctuating version of the more robust tetrahedral structure of ice. [4] However, every now and then this view has been questioned, and the debate of water structure is still ongoing (see References 5–9 and references therein).

If the structure of pure water is still a question, so is the effect on the hydrogen bond network when other components are added. The macroscopic effects are often clearly visible, for example as changes in viscosity, conductivity, or even color. However, in the microscopic scale the effects are far less known. For example, for most molecules it is unknown how many water molecules hydrate them in aqueous solutions, or how far-reaching impact the solute can have on the structure of water.

What makes liquid water so controversial is the fact that studying liquid structure is not straightforward, because the time or length scales needed to study the fluctuating network are not easily accessible. Typical experimental methods to study water are, for example, neutron [10,11] and x-ray diffraction, [12–14] which can provide the radial distribution functions of the studied system (the average positions of the atoms compared to some reference atom). For example, the way to get even more precise radial distribution functions for ambient water has been studied recently by extending the momentum transfer range in the x-ray diffraction measurement. [15] Additionally, information on water structure can be obtained with small angle x-ray scattering, [16–19] for example

on demonstrating whether liquid water is a homogeneous [16] or not. [17] On the other hand, infrared or Raman spectroscopies are indirectly linked to the structure of water via the vibrations of the bonds, [20–23] such as in the case where the timescale of the vibrations of the bonds in liquid water were found to support the uniform, homogeneous structure for the hydrogen-bond network of water. [24] Another useful vibrational technique is nuclear magnetic resonance, [25–27] which was recently applied, for instance, to study the water-methanol mixtures at different temperatures. [28]

On their own, and especially to support the experimental results, computational methods are often used in liquid studies due to the effortless structural characterization. Typical computational method is classical molecular dynamics simulations [29, 30], in which a set of parameters, such as choice of charges to characterize the molecules, interaction methods, or thermodynamic conditions, are used to create a simulation of the liquid. As it is computationally relatively light, classical molecular dynamics has been applied to vast amount of aqueous systems, ranging from pure water to studying long polymers in water. [31, 32] Another typical computational method is ab initio molecular dynamics, [33–38] where the forces in the simulation are derived from quantum mechanical electronic structure calculations. This method allows more flexibility as, for example, chemical reactions can take place during the simulation. On the other hand, it is computationally more demanding than the empirical classical molecular dynamics. Lately, discussion on how well the ab initio methods can produce the thermodynamical quantities of pure water has been ongoing. [33–35] Additionally, there are computational methods that mix classical and quantum calculations in order to improve the results while keeping the computational load reasonable. [39–42]

In the 21st century, x-ray spectroscopic methods have become important in liquid studies. [43, 44] Besides x-ray emission [45–50] and resonant inelastic x-ray scattering, [51–53] x-ray absorption and x-ray Raman scattering provide information on the local structure of liquids. For example, x-ray absorption and x-ray Raman scattering have been used especially to characterize the structure of liquid water [17, 48, 54–61] and ice, [54, 62–66] in addition to probing the structure of aqueous mixtures. [48, 67–69] Moreover, from discussing the covalent nature of the hydrogen bond in ice, [70–72] Compton scattering has been used to extensively study liquid water and ices, [73–79] most recently in nanoconfinement, [80] aqueous mixtures and alcohols, [81–83] and it has been used to study even more complex systems, such as clathrates. [84–86]

In this thesis, x-ray Raman scattering and Compton scattering are used to study water mixtures. X-ray Raman scattering probes the unoccupied electronic states via core-electron excitation, whereas Compton scattering provides information on the ground-state electron momentum density. They both are inelastic photon-in-photon-out processes which utilize hard x-rays. Thus, as hard x-rays penetrate matter easily, the inelastic x-ray scattering methods can be used to study bulk properties and the use of vacuum environment in the experiments is not necessary. Although they do not

give direct structural information, the results are linked to the structure of the system. In the interpretation of the results, both the knowledge from previous work and computer simulations with, for example, density functional theory can help to connect the measured quantities to the structure.

The aim of this thesis is to examine the effect that different molecules, ions, or polymers have on the hydrogen-bond network of water. In order to understand the behaviour of more complex systems, such as proteins, simpler systems should be understood first. So far, even for the simplest systems, including pure water, no consensus on the local structure has been found. The different ways water can interact are introduced in the following chapter, where also the scientific debate on the specifics of each interaction is discussed. As the rest of the introductory part of the thesis, following the introduction to water, the x-ray Raman and Compton scattering theory and methods are discussed. Finally, each paper in this thesis, representing different viewpoints to the interactions of water, is summarized and the thesis is completed with concluding remarks.

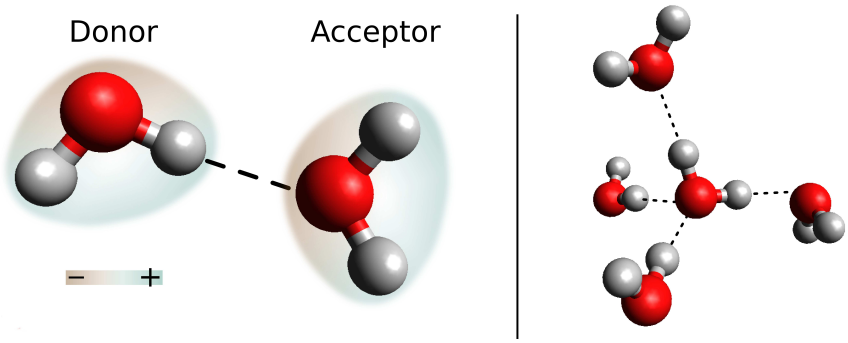

Figure 1. Left: Hydrogen bond (dashed line) between two water molecules. The polarity of the molecules makes hydrogen bonding possible (illustrated with colors). Right: A fully hydrated water molecule (in the middle) with four hydrogen bonds in a nearly tetrahedral orientation.

2 Water

Water molecules are highly interactive because they can form strong hydrogen bonds. This ability to bond makes water the complex system it is. In this section, the hydrogen-bond network of water is discussed from the structural point of view. Special emphasis is paid on how the hydrogen-bond network is altered when it is in contact with different type of molecular entities, based on the occasionally contradictory research results.

2.1 Hydrogen-bond network of water

The electric charge in water molecules is not distributed evenly in the molecule due to differences in the electronegativity of oxygen and hydrogen atoms. Thus, water molecules are polar, which makes it possible for the molecules to bond to each other by electrostatic attraction. Besides the electrostatic interaction, partial charge transfer can take place between the water molecules, which makes the bond appear as partly covalent. [87–89] Due to the intermediating hydrogen atom, the bonds created between water molecules are called hydrogen bonds (see Figure 1 for schematic presentation). It is beneficial to differentiate the molecules involved in the hydrogen bond: one covalently bonded to the bonding hydrogen is the hydrogen bond donor, while the other one is hydrogen bond acceptor (illustrated in Figure 1). Compared to different bonds, a hydrogen bond (5.5 kcal/mol) [90] is stronger than van der Waals interaction (typically of the order of 0.2 kcal/mol), but a lot weaker than covalent bonds (∼120 kcal/mol for the O-H bond in water molecule).

In a fully hydrated state water molecule can form four hydrogen bonds (Figure 1). This tetrahedral static structure is found in ice (Ih), whereas in liquid water most

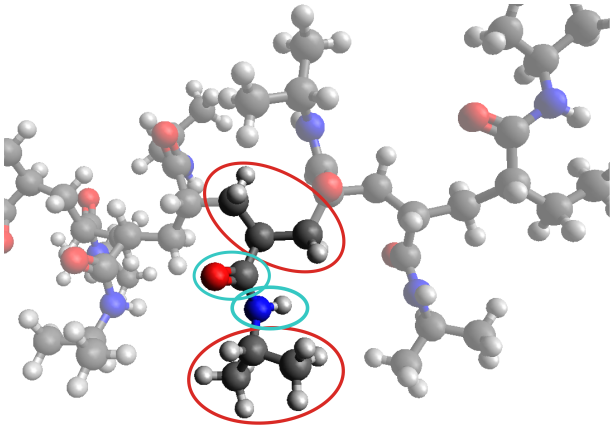

Figure 2. Hydrophilic (blue) and hydrophobic (red) groups of poly(N-isopropylacrylamide) polymer. The hydrophilic groups form hydrogen bonds with water whereas the hydrophobic groups are nonpolar and do not bond with water.

of the bonding persists,[1] but the molecules are moving and constantly forming and breaking bonds with new partners. The lifetime of a hydrogen bond in liquid water is approximately 1 ps or less, [21, 92–94] whereas broken hydrogen bonds are short-lived (less than 200 fs). [93, 95] On that account, liquid water has constantly fluctuating extensive hydrogen-bond network.

2.2 Water in solutions

The aim of this thesis is to study how the hydrogen-bond network of water changes when water is mixed with other molecules or polymers. Besides water, other molecules can also be polar and can form hydrogen bonds. This type of interaction that takes place with water via the hydrogen bonding is called hydrophilic interaction ("water loving"). On the other hand, molecules can be nonpolar and they do not form hydrogen bonds. When water interacts with nonpolar solutes the interaction is called hydrophobic interaction ("water fearing"). Compared to the intermolecular forces of the hydrophilic interaction, the hydrophobic interaction is governed by an interplay between entalphy and entropy. However, most polymers and molecules consist of both hydrophilic and hydrophobic groups, and as such they are called amphiphilic. As an example of amphiphilicity, in Figure 2 the hydrophilic and hydrophobic groups of poly(N-isopropylacrylamide) polymer are illustrated. Both hydrophiles and hy-

[1] In 2004, Wernet *et al.* suggested that liquid water would be a two-component system, with low-density water (with four hydrogen bonds per molecule) and high-density water (with two hydrogen bonds per molecule), and the high-density water would be the more dominant component. [57] Their conclusion has received opposition, and created intense discussion on the water structure which is still ongoing. [5–9, 91]

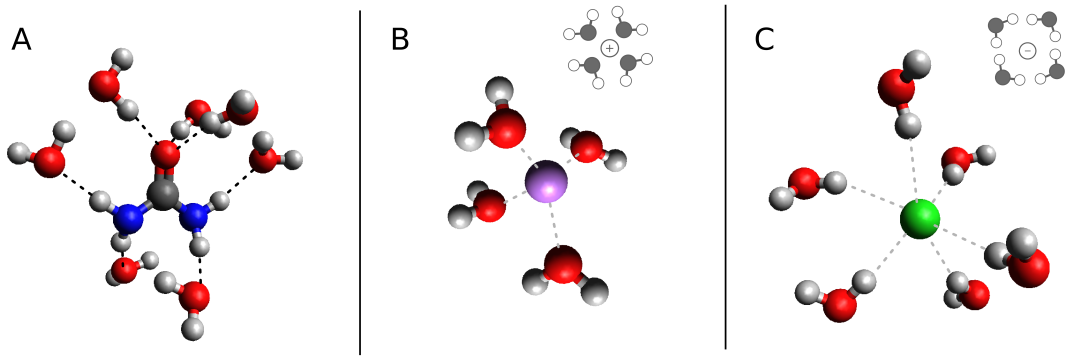

Figure 3. A) An urea molecule with seven hydrogen bonds with water molecules. B) A lithium ion with four hydrating water molecules. C) A chloride ion with six hydrating water molecules.

drophobes (and, obviously, amphiphiles) have been suggested to either enhance or disrupt the local structure of water. Enhancement or disruption of the water structure by solutes typically means in practice that the hydrating water has different number of hydrogen bonds than pure water would, or that the tetrahedral structure is altered. In the following, the different types of interactions are introduced.

2.2.1 Hydrophiles

A considerable amount of molecules or functional groups fit into the hydrophiles category. No general rules have been established on how hydrophiles affect the local structure of hydrating water, mostly due to the large variety of molecules and possible interactions. However, as they form hydrogen bonds, hydrophiles are incorporated into the hydrogen-bond network of water, but their effect on the surrounding water is dependent on the molecule in question.

Urea is one of the most studied small hydrophilic solute largely due to its usability in denaturing proteins. [96] It is highly hydrophilic, with the capability of forming up to eight hydrogen bonds with water (see Figure 3 A for a urea molecule with seven hydrogen bonds). However, the average number of hydrogen bonds per urea molecule in liquid water has been estimated to be between 2–6. [97] Urea is found to fit to the hydrogen-bond network of water, [97–100] and the dynamics of the water molecules are not found to be altered from those of bulk water. [100, 101] However, for example, discussion is still ongoing whether urea is capable of enhancing [102–104] or disrupting [105, 106] the surrounding water network. Nevertheless, with the ability of being a part of the hydrogen-bond network, urea is a good example case of hydrophiles. In this thesis, the hydrophilic interaction is playing a role in papers **II**–**IV**, as the studied systems (alcohols and poly(N-isopropylacrylamide)) have hydrophilic domains.

2.2.2 Ions

The ion-water interaction can be considered to be hydrophilic, as ions are charged particles. However, following the typical definitions of monatomic ions, in this thesis the interaction between water and ions is not called hydrogen bonding. Nevertheless, ions are easily hydrated and they are incorporated into the hydrogen-bond network of water. Depending on the charge of the ion, it interacts with either the oxygen or the hydrogen of a water molecule. Examples of possible hydration shells of lithium and chloride ions are illustrated in Figure 3 B and C, respectively. Although it has not entirely been agreed upon, the idea of how ions are actually hydrated differs from what is seen in most textbooks, where water molecules are drawn in highly ordered manner (see insets in Figures 3 B and C).

Historically, ions have been labeled as structure makers or structure breakers, based on their assumed capability to enhance or disrupt the hydrogen bond network of water. This idea stems from the Hofmeister series, in which ions are classified by their ability to affect proteins in water. [107, 108] However, as the experimental and computational methods to study the hydration of ions have improved, this type of classification has proven to be incorrect. [69, 109–115] Although the electric field of ions can be observed up to 30 Å in water, [116] long-ranging effects on water structure are not typically observed. [69, 110, 111, 117, 118] However, there are findings that the water network would be affected beyond the first hydration shell. [114, 119, 120]

Another dispute concerning ions is their hydration numbers. Although being one of the basic ways to describe the local structure, it still remains unknown how many water molecules surround ions. For example, the most often reported hydration number for lithium is 4 (similar as is seen in Figure 3 B), but the number in fact varies between 2–6, [121–129] and the observed hydration number can also vary depending on the concentration. [130, 131] This further confirms that despite being seemingly simple systems, ionic solutions prove to be complex and difficult to study. In this thesis, the ionic interaction with water is discussed in paper **I**, where the effects LiCl has on the water structure is studied with x-ray Raman scattering.

2.2.3 Hydrophobes

In 1945, Frank and Evans suggested that water molecules would form iceberg-like structures around hydrophobic groups in order to explain the excess entropy observed in mixing. [132] However, later most studies on hydrophobes have found no indication on such formation in liquid mixtures. Conversely, in high pressures water does freeze around solutes. These structures are called clathrates, but in normal conditions this clathrate formation does not take place. [133]

Over the years, numerous studies have been conducted on how water behaves around hydrophobes and the findings are manifold. For example, some recent studies have

found evidence of an enhanced water structure. [134–136] Raschke *et al.* found in a computational study that water structure at the hydration shell of hydrophobes would be more ordered, but between the hydration shells water would be less ordered. [136] Davis *et al.* observed with Raman scattering measurements and multivariate curve resolution that for linear alcohols the hydration shell water is more tetrahedral and has stronger hydrogen bonds. However, they also observed that when temperature was increased or the hydrophobic chain was long enough, there was no enhanced structure. [134]

Otherwise, there are several studies that have found that water structure around hydrophobes is less ordered than in bulk water. [137–139] For example, from neutron scattering studies Buchanan *et al.* found that there is no indication of enhanced structure of water around methane. They concluded that in fact the structure is slightly less tetrahedral than in bulk water. [139]

An interesting notion about hydrophobes is that some results suggest that the size of the hydrophobes affects its ability to influence water structure. [140–142] Large hydrophobes, with hydrophobic surfaces that are extensive (and almost flat), break the hydrogen bonds of the water molecules, as the network cannot arrange itself without breaking bonds. On the other hand, when the size of the hydrophobe decreases, the hydrophobic surface becomes more and more curved. In this case, the hydrogen-bond network of water can be wrapped around the hydrophobe without a loss of hydrogen bonds.

Paper **II** of this thesis especially focuses on the hydrophobic interaction by studying the effect of the size of the hydrophobic group of alcohol molecules on the structure of water. The hydrophobic interaction also appears as an important factor in paper **IV**, as it is found to affect the phase transition of an aqueous polymer.

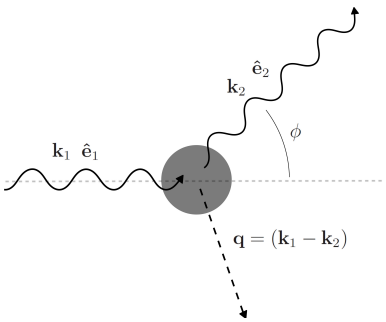

Figure 4. Schematic presentation of the inelastic x-ray scattering process.

3 Inelastic x-ray scattering

In the methods used in this thesis, the electrons are mainly interacting with the x-rays through inelastic processes. In this section, the theoretical background for inelastic x-ray scattering is briefly discussed. Throughout the thesis, atomic units are used ($\hbar = e = m_e = c\alpha = 1$), while energies related to scattering are given in electron volts (eV) and distances in Ångströms (Å).

In the inelastic x-ray scattering process, a photon with energy ω_1, wave vector $\mathbf{k}_1$, and polarization unit vector $\hat{\mathbf{e}}_1$ scatters from the target, which is initially in state $|I\rangle$ with energy E_I, leaving it in final state $|F\rangle$ with energy E_F. The scattered photon has energy ω_2, wave vector $\mathbf{k}_2$, and polarization unit vector $\hat{\mathbf{e}}_2$, and it is scattered to an angle ϕ. Thus, energy $\omega = (\omega_1 - \omega_2)$ and momentum $\mathbf{q} = (\mathbf{k}_1 - \mathbf{k}_2)$ are transferred to the target (see Figure 4).

In the non-relativistic limit, the double-differential scattering cross-section for non-resonant inelastic x-ray scattering, [143]

$$\frac{d^2\sigma}{d\Omega d\omega_2} = \left(\frac{d\sigma}{d\Omega}\right)_{\mathrm{Th}} S(\mathbf{q}, \omega), \tag{1}$$

consists of two factors: the Thomson scattering cross section, which is only dependent on the experimental set-up,

$$\left(\frac{d\sigma}{d\Omega}\right)_{\mathrm{Th}} = r_0^2 \left(\frac{\omega_2}{\omega_1}\right) |\hat{\mathbf{e}}_1 \cdot \hat{\mathbf{e}}_2|^2, \tag{2}$$

where r_0 is the classical electron radius, and the dynamic structure factor

$$S(\mathbf{q}, \omega) = \sum_F \left| \langle F | \sum_l e^{i\mathbf{q}\cdot\mathbf{r}_l} | I \rangle \right|^2 \delta(E_F - E_I - \omega), \tag{3}$$

where the latter summation is over all electrons in the system at the positions $\mathbf{r}_l$. The dynamic structure factor contains all the material-dependent information of the system.

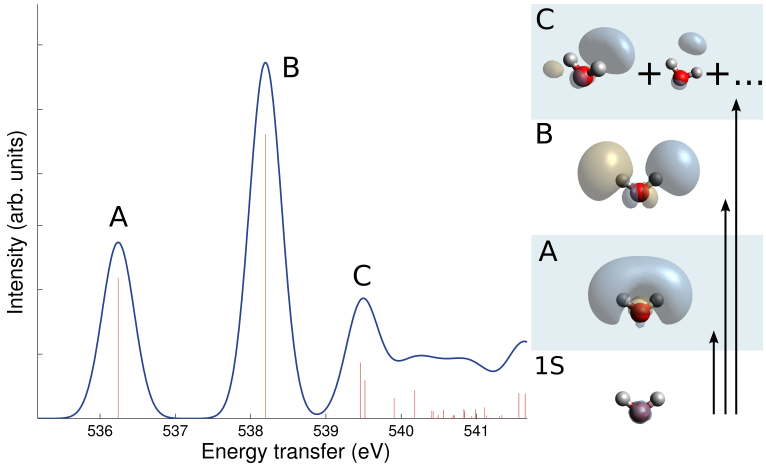

Figure 5. Computational oxygen K-edge spectra for an isolated water molecule. The figures on the right hand side represent the transitions from ground state (1S) to excited states: A for the LUMO $4a_1$ orbital, B for the LUMO+1 $2b_2$ orbital and C for higher unoccupied molecular orbitals. The transitions and orbitals are calculated with the ERKALE code. [144, 145]

The dynamic structure factor can reveal information on different processes. Whichever process dominates the $S(\mathbf{q}, \omega)$ depends on the transferred energy ω and momentum $\mathbf{q}$, which can be controlled by the choices in the experimental set-up. In this work, two different inelastic x-ray scattering methods are used, and in the following the basics of the methods are recalled.

3.1 X-ray Raman scattering

When the transferred energy ω is near the core binding energies, i.e., the ionization energies of an electron in a certain orbital, a significant contribution to the dynamic structure factor comes from a process called x-ray Raman scattering. For the x-ray Raman scattering the dynamic structure factor in the single-particle excitation picture is

$$S(\mathbf{q}, \omega) = \sum_f \left| \langle f | e^{i\mathbf{q}\cdot\mathbf{r}} | i \rangle \right|^2 \delta(E_f - E_i - \omega), \tag{4}$$

where the initial state $|i\rangle$ is a core orbital in the ground state of the system and the final states $|f\rangle$ are final orbitals in the presence of the core hole, i.e., the unoccupied molecular orbitals of the system. The energies E_i and E_f are the orbital energies corresponding to the initial and final states. In Figure 5, the x-ray Raman scattering process is presented for the oxygen K-edge for an isolated water molecule. Sharp transitions can be seen for the excitations to the lowest unoccupied molecular orbital (LUMO), and to the second unoccupied orbital (LUMO+1), followed by contribution of excitations to multiple higher-energy molecular orbitals.

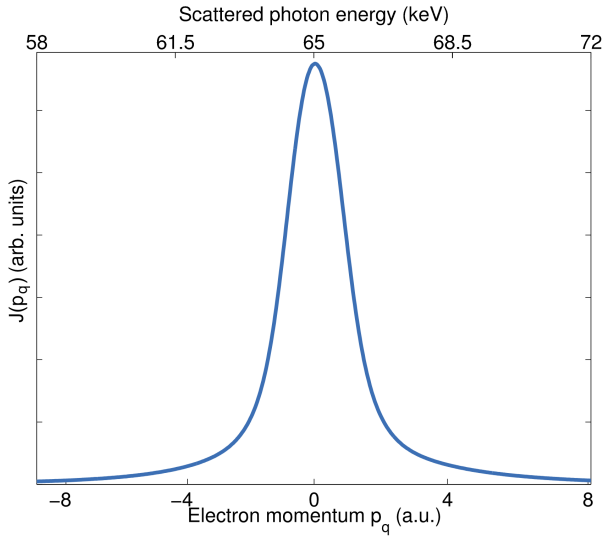

Figure 6. Compton profile of aqueous poly(N-isopropylacrylamide). The incident photon energy was 87 keV and the scattering angle 163.3°.

For small values of $|\mathbf{q}|$ the exponential in equation 4 can be expanded:

$$e^{i\mathbf{q}\cdot\mathbf{r}} \approx 1 + i\mathbf{q}\cdot\mathbf{r} + ... \tag{5}$$

Thus, most of the contribution to $S(\mathbf{q},\omega)$ arises from dipole transitions ($\langle f|\mathbf{r}|i\rangle$) at small values of $|\mathbf{q}|$. This makes x-ray Raman scattering comparable to x-ray absorption spectroscopy, where only the dipole transitions are probed. However, compared to x-ray absorption, x-ray Raman scattering is beneficial in many ways. The incoming energies can be chosen to be nearly arbitrarily high, and thus the penetration depth is much larger, making studies of bulk materials possible. Additionally, the experiments for x-ray absorption at the oxygen K-edge require vacuum as the low-energy x-rays are absorbed by air, which makes the experiments more difficult. With x-ray Raman scattering, absorption by air is low, as the incoming and scattered photons belong to the hard x-ray range (>10 keV).

Moreover, with x-ray Raman scattering it is possible to study transitions beyond the dipole transitions, as the magnitude of $\mathbf{q}$ can be adjusted. The possibilities of obtaining additional information by using large momentum transfers have been extensively studied. [146–149] However, in this thesis, the momentum transfers are restricted to values that are small enough to make the x-ray Raman scattering results comparable to x-ray absorption results.

3.2 X-ray Compton scattering

In the high energy transfer ω and high momentum transfer $|\mathbf{q}|$ region, the dominating contribution to the dynamic structure factor $\mathrm{S}(\mathbf{q},\omega)$ originates from Compton scattering. From van Hove's idea of presenting the dynamic structure factor as a correlation of the motion of the scattering particles, [150] an important notion with respect to understanding Compton scattering can be made: with high momentum transfers, different particles scatter independently. Thus, the scattering electrons in the Compton regime are independent of each other and collective processes of the electrons are not being probed. This approximation is called the impulse approximation.

Eisenberger and Platzman [151] further refined the impulse approximation in the Compton scattering theory. They stated that when the transferred energy is substantially higher than any other energy related to the ground state of the electron, the scattering process takes place very rapidly, so the potential where the electron is moving can be regarded constant. With this approximation the dynamic structure factor reduces to

$$S(\mathbf{q},\omega) = \left(\frac{1}{2\pi}\right)^3 \int |\chi(\mathbf{p})|^2 \delta(\omega - \frac{q^2}{2} - \mathbf{q}\cdot\mathbf{p}) d\mathbf{p}, \tag{6}$$

where $\chi(\mathbf{p})$ is the Fourier transform of the ground-state wave function and $|\chi(\mathbf{p})|^2$ is the ground-state electron momentum density $N(\mathbf{p})$. When equation 6 is integrated over p_q, the electron momentum projection on $\mathbf{q}$, the dynamic structure factor becomes

$$S(\mathbf{q},\omega) = \frac{J(p_q)}{|\mathbf{q}|}, \tag{7}$$

where $J(p_q)$ is the Compton profile and p_q is the electron momentum in the direction of $\mathbf{q}$. For isotropic systems, such as liquids, the Compton profile can be expressed as

$$J(p_q) = \frac{1}{2}\int d\Omega \int_{|p_q|}^{\infty} pN(p)dp. \tag{8}$$

The momentum of the electron in the direction of the scattering vector (p_q) can be approximated with the relativistic effects taken into account as [152, 153]

$$p_q \simeq \frac{|\mathbf{q}|}{2} - \frac{(\omega_1 - \omega_2)}{c}\sqrt{\frac{1}{4} + \frac{c^4}{2\omega_1\omega_2(1-\cos\phi)}}, \tag{9}$$

where c is the speed of light.

An example of a Compton profile is shown in Figure 6, where it is presented in scattered-photon energy and electron momentum scales. Interesting features in a Compton profile arise from the delta-function in equation 6. The position of the Compton profile in the energy scale (or the Compton shift) is governed by the term $\frac{q^2}{2}$, which

depends only on the incoming photon energy and the scattering angle. The width of the Compton profile is determined by the term $\mathbf{q} \cdot \mathbf{p}$, i.e., the electron momentum in the direction of the momentum transfer.

Note to the reader about notation concerning Compton scattering: In the remaining part of the thesis, where Compton scattering is discussed (papers **III** and **IV**), an established notion is used, where the momentum of the electron p_q in an isotropic system is referred as q, which should not be confused with the momentum transfer discussed in this section.

4 Methods

In order to perform an inelastic x-ray scattering experiment that requires high energy resolution with high statistical accuracy, x-ray sources with very high brilliance have to be utilized. Thus, the inelastic x-ray scattering experiments are performed at third-generation synchrotron sources with specialized instrumentation. Additionally, for interpreting the experimental data, theoretical calculations are needed in order to connect the measured spectra to molecular structures. In this section, the experimental setups are introduced, followed by short explanation on the calculations. Finally, the analysis and interpretation of the results are discussed.

4.1 Experiments

The experiments in this thesis were performed at the European Synchrotron Radiation Facility (ESRF) apart from the experiment in paper **III**, which was performed at the SPring-8 synchrotron radiation source. Detailed explanation of the BL08W beamline at SPring-8 can be found in Reference 154. In the following, the setups of the two beamlines used at ESRF are discussed.

4.1.1 Experimental setup at beamline ID16 (ESRF)

The high-resolution inelastic x-ray scattering beamline ID16 was used in the x-ray Raman scattering experiments.[2] [155] At ID16, the x-rays were produced by the storage-ring electrons with three undulators. The undulator radiation was monochromatized by two monochromators: a Si(111) double-crystal monochromator and a Si(440) channel-cut monochromator, which further refined the bandwidth. The monochromatized radiation was focused with a Rh-coated toroidal mirror. The spot sizes in the experiments in this thesis were $150 \times 50\mu m^2$ and $100 \times 30\mu m^2$ (papers **I** and **II**).

The intensity of the incoming beam was monitored with Si pin diode before the sample. The scattered beam was energy analyzed with nine spherically bent Si(660) analyzer crystals and collected with a Medipix2 pixel detector in a Rowland circle geometry. This combination created a possibility of imaging the origin from the scattered x-rays inside the sample along the beam. [156] This could be used to effectively remove the background scattering from the signal originating from the sample. The x-ray Raman scattering spectrum was measured by keeping the analyzer energy fixed and scanning the incident photon energy. The total energy resolution obtained in the experiments at ID16 were 0.5 eV and 0.57 eV (papers **I** and **II**).

[2]Inelastic x-ray scattering beamline ID16 was closed for operation in 2012 and the inelastic x-ray scattering spectroscopy research continues at the new beamline ID20 as a part of the ESRF upgrade programme.

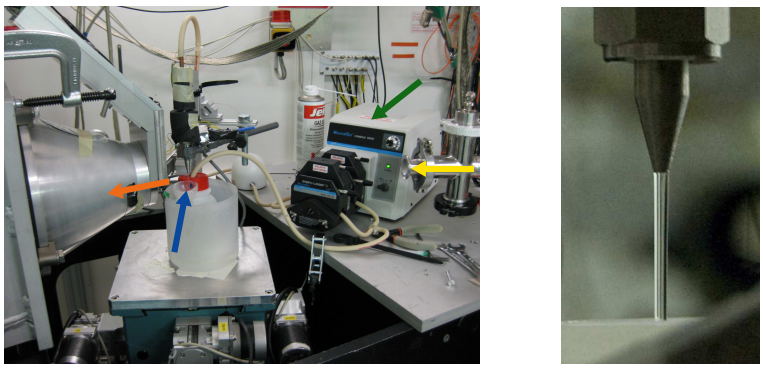

Figure 7. Left: Experimental liquid flow setup at beamline ID16. The liquid column (sample) is indicated with blue arrow, whereas the peristaltic pump is indicated with green arrow. The incoming and scattered beams are indicated with yellow and orange arrows. Right: Close-up of the nozzle and the sample.

4.1.2 Experimental setup at beamline ID15B (ESRF)

Beamline ID15B [157] can be used for Compton scattering experiments. At ID15B, the x-rays are produced by the storage-ring electrons with a seven-period asymmetric multipole permanent-magnet wiggler. Horizontally focusing bent Laue-crystal monochromators are used and the incident intensity is monitored with a Si pin diode.

High statistical accuracy is needed for Compton scattering experiments as the changes in the Compton profiles are small. Hence a 13-element Ge solid state detector is used to detect the scattered photons. Each of the detectors has their own electronics. Although the Ge solid state detector does not achieve as good momentum resolution as high-resolution scanning crystal spectrometers described in Reference 157, for liquid water systems the need for high statistical accuracy outweighs the requirement for a high momentum resolution. [82] The momentum resolution obtained in the Compton scattering experiment (paper **IV**) was 0.64 a.u. while the observed statistical difference at the Compton peak ($p_q = 0$ a.u.) was less than 0.1% of the peak height.

4.1.3 Sample environments

In order to avoid radiation damage to the sample, [158, 159] in the x-ray Raman scattering experiments the samples are contained in a peristaltic-pump based closed-loop setup (see Figure 7). With the setup, a stable vertical liquid column (diameter 2 mm) is produced from a stainless steel nozzle. In this set up, the sample is being constantly renewed and thus the radiation exposure to a specific volume is reduced.

Due to the small quantity of available sample, the liquid flow setup could not be used in the x-ray Compton scattering experiment (paper **IV**), and thus a different type of sample environment was used. In this case, the sample was in a 2 mm diameter borosilicate glass capillary with 10 μm thick walls connected with copper sample holder

to a cryostat which controlled the temperature of the system. The system was in a vacuum chamber with 25 μm thick Mylar windows to remove the air from the vicinity of the sample.

4.2 Calculations

Calculation of the x-ray Raman spectrum or Compton profile from a modeled system can help to connect the experimental spectra to molecular structures. In this section, the computational methodology is briefly discussed.

In order to computationally obtain a Compton profile or an x-ray Raman spectrum, information on the electronic structure is needed. The computational approach assumes the Born-Oppenheimer approximation, [160] where the nuclei are considered to form an external potential for the electrons. The electrons of the system should be described by a many-body wave function that satisfies the Schrödinger equation. However, solving such a problem for realistic system with many electrons is unfeasible, and approximations are needed.

In density functional theory, [161, 162] the energy of the system is a functional of the electronic density $\rho(\mathbf{r})$ instead of the wave function. In order to construct the electronic density, Kohn and Sham introduced a methodology with a fictitious set of noninteracting electrons, with their orthogonal wavefunctions, $\phi_i(\mathbf{r})$, equaling the electronic density, $\rho(\mathbf{r}) = \sum_i |\phi_i(\mathbf{r})|^2$, summed over all of the electrons. [163] The Kohn-Sham wavefunctions satisfy the Kohn-Sham Schrödinger equation

$$\left(-\frac{1}{2}\nabla^2 + V_{\mathrm{KS}}(\mathbf{r})\right)\phi_i(\mathbf{r}) = \epsilon_i\phi_i(\mathbf{r}), \tag{10}$$

where ϵ_i are the Kohn-Sham eigenvalues corresponding to the Kohn-Sham orbitals $\phi_i(\mathbf{r})$, and the potential is given by

$$V_{\mathrm{KS}} = V_{\mathrm{ext}}(\mathbf{r}) + \int \frac{\rho(\mathbf{r}')}{|\mathbf{r}-\mathbf{r}'|}d\mathbf{r}' + V_{\mathrm{xc}}(\mathbf{r}). \tag{11}$$

The potential is a sum of the external potential due to a set of nuclei $V_{\mathrm{ext}}(\mathbf{r})$, the mean-field of all the electrons (called Hartree potential), and the exchange-correlation potential $V_{\mathrm{xc}}(\mathbf{r})$. The exchange due to Pauli repulsion and correlation due to Coulombic interactions beyond the mean-field Hartree potentials are approximated in the calculations (for approximations see, for example, References 163–169).

When the exchange-correlation is approximated and an initial density for the system is given, the Kohn-Sham equations can be iteratively solved to produce the electronic density. According to the formal construction of the theory, the Kohn-Sham orbitals can only be used to create the electron density. However, in practice, the orbitals are often considered to represent single-particle wave functions, [170] and the energies

are considered to be orbital energies and used to calculate, for example, the excitation energies. [171] For the Compton scattering calculations, the electron momentum density is obtained as a sum of the Fourier transformed Kohn-Sham orbitals. [172]

In this thesis, the density functional theory calculations are performed with the StoBe-deMon code [173] (papers **I** and **III**) and with the ERKALE code [144, 145] (papers **II** and **IV**). Details of each calculation are found in the papers. For the x-ray Raman calculations the transition-potential approximation was used. [174] Essentially in this approximation, following the Slater's transition state approximation, [175] half an electron is in the core state, but the unoccupied molecular orbitals are kept unoccupied. This reduces the amount of calculations needed, as one calculation is performed instead of calculating the transitions from a core orbital to the excited orbitals. [176,177]

The spectral calculations are done with small molecular clusters. Thus, it is required to have structures that would resemble real situations as well as possible. There are multiple ways to obtain such structures, but in this thesis classical molecular dynamics simulations [29] are used. In principle, classical molecular dynamics is a simulation of the movement of atoms or molecules. Each atom is assigned a force field (a potential), and the atoms interact with each other. Sequentially, in small time steps, the forces are calculated, and the atoms are moved accordingly. In a nutshell, classical molecular dynamics is a numerical method to solve Newton's equations of motion.

For the classical molecular dynamics simulations the Gromacs software [178] is used with OPLS-AA [179] and TIP4P [180] force fields. Exception is made in the case of aqueous LiCl (paper **I**), where modified OPLS-AA force field is used for Li and Cl ions to correct the error arising from the lack of polarizability in the water force field. The rest of the simulation details are described in the papers. From the simulations small roughly spherical clusters (with radius of 4–6 Å) were randomly selected for the density functional theory calculations. In paper **III**, the clusters are further modified to obtain more precise information. To connect the spectra from calculated static clusters to the experimentally measured dynamical system, the spectra are calculated for a set of at least hundred clusters, thus generating random variety to the structures.

4.3 Analysis and interpretation

In the case of inelastic x-ray scattering, careful data analysis of the measured spectra should always be made as the differences in the measured quantities are often small. Here selected points about the data analysis are reviewed. More detailed explanation of all the aspects of data analysis can be found in literature (for example, for Compton scattering, see Reference 181, and for x-ray Raman scattering, Reference 182). Description of the individual choices done in the data analysis in this thesis can be found in the papers.

As described in the Section 4.1, the x-ray Raman experiments are done using a crys-

tal spectrometer in the so-called inverse scanning geometry, where the analyzer energy is fixed and the incident photon energy is scanned. The x-ray Raman spectrometer has a capability of real-space imaging of the sample, [156] which produces not only spectra, but at the same time images of the beam path within the sample and its environment as well. The region of interest within the aquired images can be selected for the data analysis, and thus only the signal from the sample (and not the sample holder or environment) is analyzed further. The collected spectra are normalized to the incident photon flux, and the spectra of each analyzer are shifted to a common energy-transfer calibration and interpolated to the same energy grid. Energy-dependent corrections are needed in the data analysis. Most notable is the absorption on the path of the beam between the incident-flux monitor and the sample. The analyzer energy is kept fixed during the experiments, which removes the concern about the energy-dependence of the spectrometer efficiency. Background from valence electrons (Compton or plasmon) must be removed from the spectra. This is typically done by subtracting a suitable monotonically varying function from the spectra. Finally, the spectra are normalized to equal area in a specific energy range.

The Compton scattering experiments are done using a Ge solid state detector, which yields spectra through a multichannel analyser electronics. In the Compton scattering experiments, the spectra are acquired repeatedly, each one integrated for a few minutes. First the different spectra of the individual detectors are shifted to match in energy scale and summed together. The energy scales of the detectors are determined by x-ray fluorescence from a known calibration sample. In the Compton data analysis, the absorption corrections are also needed. Additional energy-dependent corrections arise from the detector efficiency and the scattering cross section. Multiple scattering correction is taken into account when processing the Compton profiles. The background is measured from an empty sample cell, and subtracted from the Compton profiles. The Compton profiles are normalized to the number of electrons in the system before summing the results from different detectors together. Finally, the symmetric negative and positive sides of the Compton profile are averaged.

When the data analysis and computational work has been done, begins the most interesting part of scientific work – interpretation of the results. In the following sections, the current general ideas for the interpretation of the oxygen K-edge spectra and Compton profiles are discussed.

4.3.1 Oxygen K-edge spectra

In the discussion of the oxygen K-edge spectrum typically three different regions are examined: the pre-edge ($E \approx 535$ eV), the main-edge ($E \approx 538$ eV), and the post-edge ($E \approx 540 - 542$ eV) (illustrated in Figure 8). The spectrum depends on the molecular structure of the scattering system, but the correlation is not straightforward. Nevertheless, some interdependence has been observed. Typically, the increase in the intensity in

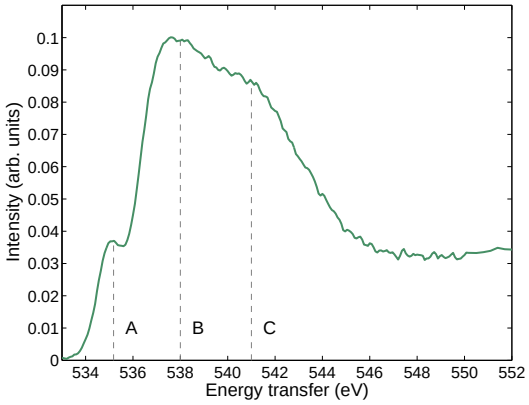

Figure 8. X-ray Raman spectrum at the oxygen K-edge for pure water, with pre-edge (A), main-edge (B), and post-edge (C).

the pre-edge area is connected to breaking or weakening of hydrogen bonds. [54,66,183] On the other hand, increased intensity in the post-edge is related to the tetrahedral ordering of the system (as in hexagonal ice), [57, 62, 63, 66] whereas the main-edge is enhanced when density increases, i.e., the scattering molecule has more (nonbonded) near neighbours. [183–185] However, the spectral changes are rarely independent of each other and typically changes are seen in more than one region. For example, when water is heated, the pre-edge is increased and the post-edge is decreased while the main-edge remains unchanged. [17, 56] In comparison, when pressure is increased in water, the pre- and post-edges remain unchanged, but changes are seen in the main-edge. [66,186]

Additionally, a good estimation on the experimental sensitivity of geometrical changes can be drawn from the work by Pylkkänen *et al.* [56] They studied the oxygen K-edge spectra for liquid water in different temperatures and in normal pressure with an experimental setup corresponding to those in this thesis (papers **I** and **II**). In their work, two spectra are distinguishable if the temperature difference is approximately 20 °C. Thus, the structural changes needed to take place in the studied system have to be of the order of the changes taking place when the temperature of liquid water is altered 20 °C in order to observe changes in the oxygen K-edge spectra.

The energetics of the system can give a rough estimate on the change in amount of hydrogen bonds. In the liquid water range (0–100 °C), the total energy absorbed is approximately 1.8 kcal/mol when water is heated from 0 °C to 100 °C. On the other hand, the enthalpy of fusion for water (ice Ih to water at 0 °C) is 1.4 kcal/mol. In contrast, the enthalpy of vaporization is 9.7 kcal/mol (liquid to gas at 100 °C). Thus, the changes upon heating liquid water over the whole range are of the same order than upon melting of ice. In ice (Ih) each water molecule has four hydrogen bonds, whereas for liquid water (at low temperatures) the number of hydrogen bonds is estimated to be, on average, 3.4–3.6 per molecule. Thus, the number of broken bonds upon melting is approximately 0.5 bonds per molecule. Smallest changes that can be seen in the spectra

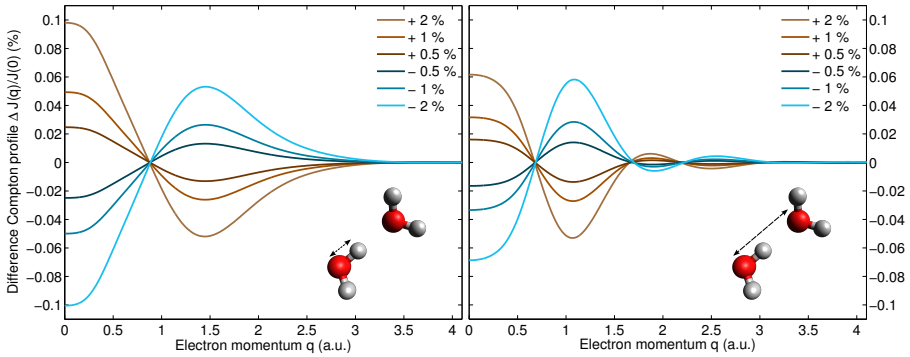

Figure 9. Example difference Compton profiles for water dimer. On the left hand side are the difference Compton profiles with changes in the covalent O-H bond length and on the right hand side are the difference Compton profiles with changes in the O..O hydrogen bond length.

thus correspond to a change of 0.1 hydrogen bonds per molecule (approximately the same amount as in 20 °C temperature difference). This corresponds to 1 fully broken hydrogen bond in 35 water molecules at room temperature.

From previous work, rough guidelines on the magnitude of the changes observable with x-ray Raman scattering can be concluded. Additionally, previous work gives some starting points to the interpretation of the spectra. In more complex compounds, especially those which include oxygen in addition to the oxygen in the water molecules, the spectral features cannot be interpreted as simply. Overall, in all interpretations, understanding the system is important and attention must be paid to the specifics of the studied case.

4.3.2 Compton scattering

Similarly to x-ray Raman scattering, Compton scattering does not represent directly any structural quantities of the studied system although Compton profiles depend on the structure of the system. Thus, the interpretation of the results is not straightforward and model calculations are important. Hakala *et al.* [77, 82, 187] and Nygård *et al.* [74–76] have done extensive work on how to interpret the Compton scattering results for water.

According to Hakala *et al.*, [187] the most notable local structural changes in liquid water systems reflected in the Compton profiles arise from changes in covalent bond lengths and the intermolecular distances. In order to illustrate these changes, a test calculation for altering the covalent bond length (O-H participating in the hydrogen bond) and oxygen-oxygen (hydrogen bond) length for water dimer is shown in Figure 9. The O-H bond lengths are originally 0.985 Å and O..O bond length 2.763 Å and the Compton profiles are calculated with the ERKALE code. The difference Compton profiles for changes in intra- and intermolecular lengths vary quite notably. The dif-

ference Compton profile for a change in the covalent bond length has a broad shape, with signal clearly deviating from zero to high momentum (∼3 a.u.). However, for intramolecular change the resulting difference Compton profile has high-frequency oscillations that approach zero at lower momentum. These examples are in line with the results of Hakala *et al.* [187]

These models are done for small systems, but the basic principle is generally also observed for larger systems. Typically, the differences in Compton profiles are caused by density variations, for example, when temperature is altered, [74, 75, 85] or in different ice phases [79]. Alternatively, the differences can arise from changes in covalent bond lengths, for example, when hydrogen in water was replaced with deuterium (thus affecting the bond lengths). [75] However, in most cases both of these effects are observed. Even though these intra- and intermolecular signatures can be thought as a rule of thumb, it is always advisable to perform extensive calculations to match the studied system as well as possible.

5 Summary of papers

In the following, the four papers of the thesis are presented. They describe example cases for the different ways water can interact. In the first two papers, the structural changes in water are observed with x-ray Raman scattering, whereas in the following two, Compton scattering is used to characterize the systems. In the first paper (**I**), the hydration of ions is studied. In paper **II**, the hydrophobic interaction is studied with alcohol molecules with varying length of the hydrophobic group. In paper **III**, the solvation of ethanol molecules is studied from the Compton scattering point of view. The fourth paper (**IV**) describes the structural changes of a self-arranging polymer in water.

5.1 Saturation Behavior in X-ray Raman Scattering Spectra of Aqueous LiCl (Paper I)

Many questions regarding the hydration of ions are debated. For example, the effect ions have on the hydrogen-bond network of water or on the structure of the first hydration shell (both in terms of number of molecules or their arrangement) are not agreed upon. LiCl is highly soluble to water (up to 2.5 water molecules per one ion), which makes it a good candidate to study the disruption of the hydrogen-bond network as the concentration of the ions can be gradually increased to high concentrations. In this work, changes in the hydrogen-bond network are studied with x-ray Raman scattering in a concentration range of 0–17 M (mol of LiCl / kg of water).

The oxygen K-edge spectra are observed to change linearly until the concentration of approximately 11 M (equivalent to 5 water molecules per ion pair) after which the spectra saturate. One would assume to see some nonlinearity at a concentration of approximately 5 M, where stoichiometrically all the water molecules are on the hydration shells of the ions. However, at this point nothing special is observed in the spectra. On the other hand, concerning hydrogen bonds, the numbers are more logical: at 5 M there are 44 hydrogen-bond donors and acceptors per ion pair whereas at 11 M there are only 20 left. Depending on how many hydrogen bonds are broken on the first hydration shell of ions, [114, 121–131, 188–190] 6–13 donors or acceptors per ion pair are left for water-water interactions at 11 M, whereas approximately 30 are left at 5 M. Thus, the hydrogen-bond network can be altered linearly until a concentration at which almost no network is left to break.

The results in this article suggest that there are no long-range effects on the hydrogen-bond network because the saturation concentration is so high. Thus, in conclusion, ions only affect water molecules at their first hydration shell and are not capable of destroying (or creating) structure at longer distances.

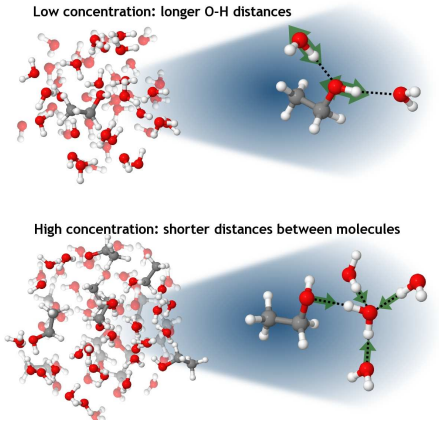

Figure 10. Schematic illustration explaining the findings of Paper **III**.

5.2 Effect of the Hydrophobic Alcohol Chain Length on the Hydrogen-Bond Network of Water (Paper II)

Alcohol molecules are practical to study the hydrophilic and hydrophobic effects. Small linear alcohols have the same hydrophilic OH group and they form similar hydrogen bonds with water molecules. However, the hydrophobic hydrocarbyl chain length increases from methanol to propanol. Hence the hydrophobic interaction volume increases for longer alcohols. In this x-ray Raman scattering study, the small linear alcohols are mixed with water in the same mole fractions in order to investigate the effects of the increasing hydrophobic interaction. The mole fractions are 5% and 15%, which correspond to 15 vol-% and 37 vol-% in ethanol-water mixtures. Thus, the surface area between the alcohols and water is substantial, but most of the oxygen K-edge signal comes from water molecules.

Surprisingly, no changes are observed in the oxygen K-edge spectra beyond a superposition of signals from oxygen in alcohols and in water. Thus, the results suggest that alcohols do not alter the hydrogen-bond network substantially. The work concludes that, upon hydration of alcohol molecules, there is no change in the number of hydrogen bonds, nor is the tetrahedrality of water molecules changed.

5.3 Measurement of Two Solvation Regimes in Water-Ethanol Mixtures Using X-Ray Compton Scattering (Paper III)

In this work, water-ethanol mixtures are studied in different concentrations with x-ray Compton scattering. When the Compton profile of the mixtures are compared to the Compton profiles of pure liquids (in equivalent weights), two distinct difference Compton profiles are obtained. The low concentration (5.5 mol-%) difference Compton profile deviates from those of high concentrations (15.7 to 73.1 mol-%). With the help

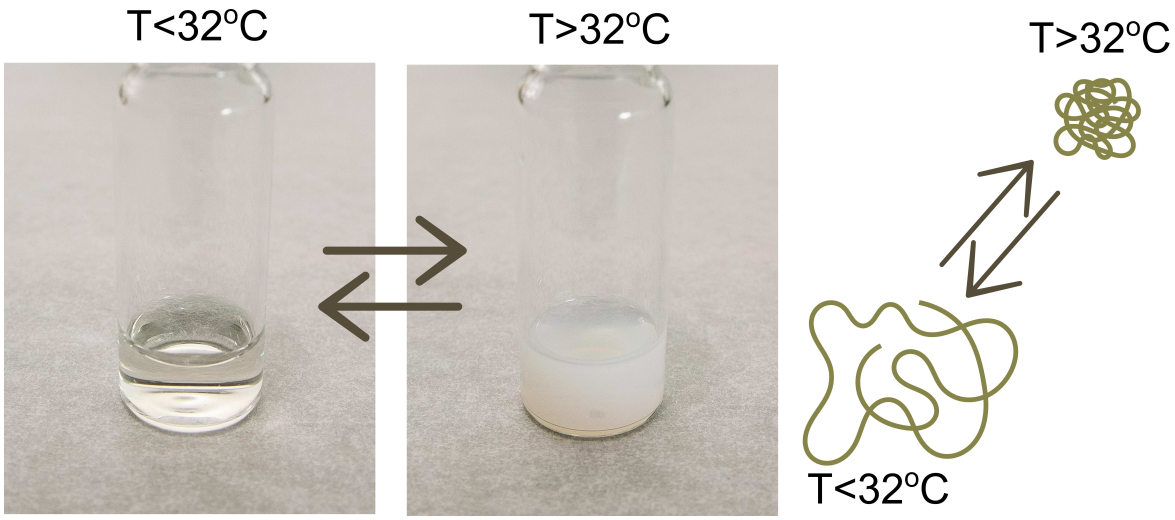

Figure 11. Aqueous PNIPAM in swollen hydrophilic state (left) and collapsed hydrophobic state (right). Far right is a schematic illustration of the coil-to-globule transition.

of density functional theory calculations, the changes in the Compton profiles can be identified to mainly arise from two geometrical changes in the liquid (see Figure 10). At low concentration, the mixture has elongated covalent bond lengths compared to those of pure liquids. However, at high concentrations, a density increase of the mixture is observed. This is a commonly known phenomenon: 1 unit volume of water and 1 unit volume of ethanol equal less than two unit volumes of water-ethanol mixture. However, it is surprising that at low concentration the bond length elongation is observed instead.

One can readily compare this work to results of paper **II**, where no changes are observed in the x-ray Raman scattering spectra for water-ethanol mixtures in concentrations between 5 and 15 %. This highlights the different type of information obtainable with Compton and x-ray Raman scattering and how sensitive Compton scattering is for the changes in the covalent bond lengths.

5.4 Molecular-Level Changes of Aqueous Poly(N-isopropylacrylamide) in Phase Transition (Paper IV)

Aqueous poly(N-isopropylacrylamide) (PNIPAM) is a self-arranging thermoresponsive polymer. In water at approximately 32 °C PNIPAM changes its conformation from a swollen hydrophilic state to a collapsed hydrophobic state (see Figure 11). The transition is reversible, and it can be observed visually. The side chain of PNIPAM has groups that can form hydrogen bonds with water molecules and it also has hydrophobic domains (see Figure 2 on page 5). Additionally, the carbonyl group (C=O) accepts up to two hydrogen bonds and the amine group (N-H) donates one hydrogen bond. Therefore, a long PNIPAM polymer can form hydrogen bonds with itself. It is proposed

that upon the phase transition the hydrogen bonding between PNIPAM and water reduces and PNIPAM starts to form intrachain hydrogen bonds. [191–198] Additionally, the hydrophobic parts of PNIPAM affect the phase transition. [32, 192, 199, 199–202]

In this paper, the phase transition of PNIPAM is studied with Compton scattering. When the experimental difference Compton profile is compared with computationally obtained Compton profiles for certain type of changes, the results show that in the phase transition of aqueous PNIPAM two changes takes place: there is an increased amount of broken hydrogen bonds and the covalent bond lengths are elongated. The results demonstrate the complexity of the system, as these two changes are contradictory in simple systems (weakening of hydrogen bonds is usually related to the contraction of the covalent bond lengths). The results indicate that the hydrophobic interaction is important in the phase transition as the breaking of the hydrogen bonds cannot on its own explain the two observed changes.

6 Concluding remarks

Despite profound work, the structure of liquid water in solutions still remains ambiguous, although the solvating properties of water have been observed to have major importance in nature. Thus, new information with inelastic x-ray scattering is valuable. As inelastic x-ray scattering methods lack the typical challenges of liquid studies using x-rays (for example, sensitivity to surface or need for vacuum environment), nearly routine experiments on liquids can be conducted.

Four experiments on aqueous solutions were presented in this thesis as examples of different interactions in water. With x-ray Raman scattering the structure of the hydrogen bond network of water was observed only to be altered in the first hydration shell of the ions, despite the long range to which the charge of the ions can be detected in water. Additionally, x-ray Raman scattering was used on alcohol-water mixtures to study the hydrophobic interaction. The oxygen K-edge spectra were observed to remain unaltered upon addition of alcohols, which suggests that the hydrophobic interaction does not affect the hydrogen-bond network of water. Water-ethanol mixtures were further studied with Compton scattering, which confirmed that no alteration on hydrogen bonding occurs. As Compton scattering is extremely sensitive to the changes in the covalent bonds, at low concentrations elongation of the intramolecular bond lengths was observed. The final studied system included in this thesis is a self-arranging aqueous polymer, poly(N-isopropylacrylamide). The study underlined the sensitivity of the Compton scattering to internal bond lengths as upon the phase transition overall bond lengths were observed to elongate and hydrogen bonds break. This finding emphasizes the importance of the hydrophobic interaction in the phase transition.

Overall, the experiments in this thesis demonstrate the complexity of the water systems. There is no universal truth on how water structure is altered when interacting with other components – the systems have their own unique response. The experiments indicate that water is flexible and capable of adapting to new circumstances. They also show the importance of obtaining information with different techniques: by combining knowledge a better picture can be achieved.

The inelastic x-ray techniques are constantly improving. The beamlines and x-ray sources keep becoming better, while computational capacities continue to grow, with more and more codes being developed specifically to the needs of inelastic x-ray scattering. Thus, in the future, the details of water structure can be assessed even more precisely. With insightful planning of the experiments, important steps can be taken towards the ultimate goal of understanding water.

References

[1] I. Langmuir, Molecular Layers. Pilgrim Trust Lecture. *Proc. R. Soc. London, Ser. A* **170**, 1 (1939).

[2] P. Ball, Water as an Active Constituent in Cell Biology. *Chem. Rev.* **108**, 74 (2008).

[3] B. Alberts, A. Johnson, J. Lewis, M. Raff, K. Roberts, and P. Walter, editors, Molecular Biology of the Cell, 4th edition. Garland Science, New York (2002).

[4] J. D. Bernal and R. H. Fowler, A Theory of Water and Ionic Solution, with Particular Reference to Hydrogen and Hydroxyl Ions. *J. Chem. Phys.* **1**, 515 (1933).

[5] G. N. I. Clark, C. D. Cappa, J. D. Smith, R. J. Saykally, and T. Head-Gordon, The Structure of Ambient Water. *Molecular Physics* **108**, 1415 (2010).

[6] A. Nilsson and L. G. M. Pettersson, Perspective on the Structure of Liquid Water. *Chem. Phys.* **389**, 1 (2011).

[7] A. K. Soper, Recent Water Myths. *Pure Appl. Chem.* **82**, 1855 (2010).

[8] R. H. Henchman and S. J. Cockram, Water's Non-Tetrahedral Side. *Faraday Discuss.* **167**, 529 (2013).

[9] A. Nilsson, C. Huang, and L. G. M. Pettersson, Fluctuations in Ambient Water. *J. Mol. Liquids* **176**, 2 (2012).

[10] A. K. Soper, The Radial Distribution Functions of Water and Ice from 220 to 673 K and at Pressures up to 400 MPa. *Chem. Phys.* **258**, 121 (2000).

[11] A. K. Soper, F. Bruni, and M. A. Ricci, Site-Site Pair Correlation Functions of Water from 25 to 400 °C: Revised Analysis of New and Old Diffraction Data. *J. Chem. Phys.* **106**, 247 (1997).

[12] J. M. Sorenson, G. Hura, R. M. Glaeser, and T. Head-Gordon, What Can X-ray Scattering Tell us About the Radial Distribution Functions of Water? *J. Chem. Phys.* **113**, 9149 (2000).

[13] G. Hura, J. M. Sorenson, R. M. Glaeser, and T. Head-Gordon, A High-Quality X-ray Scattering Experiment on Liquid Water at Ambient Conditions. *J. Chem. Phys.* **113**, 9140 (2000).

[14] A. H. Narten and H. A. Levy, Liquid Water: Molecular Correlation Functions from X-ray Diffraction. *J. Chem. Phys.* **55**, 2263 (1971).

[15] L. B. Skinner, C. Huang, D. Schlesinger, L. G. M. Pettersson, A. Nilsson, and C. J. Benmore, Benchmark Oxygen-Oxygen Pair-Distribution Function of Ambient Water from X-ray Diffraction Measurements with a Wide Q-Range. *J. Chem. Phys.* **138**, 074506 (2013).

[16] G. N. I. Clark, G. L. Hura, J. Teixeira, A. K. Soper, and T. Head-Gordon, Small-Angle Scattering and the Structure of Ambient Liquid Water. *Proc. Nat. Acad. Sci. U.S.A.* **107**, 14003 (2010).

[17] C. Huang, K. T. Wikfeldt, T. Tokushima, D. Nordlund, Y. Harada, U. Bergmann, M. Niebuhr, T. M. Weiss, Y. Horikawa, M. Leetmaa, M. P. Ljungberg, O. Takahashi, A. Lenz, L. Ojamäe, A. P. Lyubartsev, S. Shin, L. G. M. Pettersson, and A. Nilsson, The Inhomogeneous Structure of Water at Ambient Conditions. *Proc. Natl. Acad. Sci. U.S.A.* **106**, 15214 (2009).

[18] L. Bosio, J. Teixeira, and H. E. Stanley, Enhanced Density Fluctuations in Supercooled H_2O, D_2O, and Ethanol-Water Solutions: Evidence from Small-Angle X-Ray Scattering. *Phys. Rev. Lett.* **46**, 597 (1981).

[19] R. W. Hendricks, P. G. Mardon, and L. B. Shaffer, X-ray Zero-Angle Scattering Cross Section of Water. *J. Chem. Phys.* **61**, 319 (1974).

[20] Q. Hu, X. Lü, W. Lu, Y. Chen, and H. Liu, An Extensive Study on Raman Spectra of Water from 253 to 753 K at 30 MPa: A New Insight into Structure of Water. *J. Mol. Spectrosc.* **292**, 23 (2013).

[21] H. J. Bakker and J. L. Skinner, Vibrational Spectroscopy as a Probe of Structure and Dynamics in Liquid Water. *Chem. Rev.* **110**, 1498 (2010).

[22] S. A. Corcelli and J. L. Skinner, Infrared and Raman Line Shapes of Dilute HOD in Liquid H_2O and D_2O from 10 to 90 °C. *J. Phys. Chem. A* **109**, 6154 (2005).

[23] C. J. Fecko, J. D. Eaves, J. J. Loparo, A. Tokmakoff, and P. L. Geissler, Ultrafast Hydrogen-Bond Dynamics in the Infrared Spectroscopy of Water. *Science* **301**, 1698 (2003).

[24] J. Savolainen, S. Ahmed, and P. Hamm, Two-Dimensional Raman-Terahertz Spectroscopy of Water. *Proc. Nat. Acad. Sci. U.S.A.* **110**, 20402 (2013).

[25] J. K. M. Sanders and B. K. Hunter, editors, Modern NMR Spectroscopy: A Guide for Chemists, Second edition. Oxford University Press, Oxford (1993).

[26] K. Modig, B. G. Pfrommer, and B. Halle, Temperature-Dependent Hydrogen-Bond Geometry in Liquid Water. *Phys. Rev. Lett.* **90**, 075502 (2003).

[27] T. S. Pennanen, P. Lantto, A. J. Sillanpää, and J. Vaara, Nuclear Magnetic Resonance Chemical Shifts and Quadrupole Couplings for Different Hydrogen-Bonding Cases Occurring in Liquid Water: A Computational Study. *J. Phys. Chem. A* **111**, 182 (2007).

[28] C. Corsaro, J. Spooren, C. Branca, N. Leone, M. Broccio, C. Kim, S.-H. Chen, H. E. Stanley, and F. Mallamace, Clustering Dynamics in Water/Methanol Mixtures: A Nuclear Magnetic Resonance Study at 205 K $<$ T $<$ 295 K. *J. Phys. Chem. B* **112**, 10449 (2008).

[29] M. P. Allen and D. J. Tildesley, editors, Computer Simulation of Liquids. Oxford University Press, Oxford (2009).

[30] B. Guillot, A Reappraisal of What We Have Learnt During Three Decades of Computer Simulations on Water. *J. Mol. Liq.* **101**, 219 (2002).

[31] D. Bandyopadhyay, S. Mohan, S. K. Ghosh, and N. Choudhury, Correlation of Structural Order, Anomalous Density, and Hydrogen Bonding Network of Liquid Water. *J. Phys. Chem. B* **117**, 8831 (2013).

[32] S. A. Deshmukh, Z. Li, G. Kamath, K. J. Suthar, S. K. R. S. Sankaranarayanan, and D. C. Mancini, Atomistic Insights into Solvation Dynamics and Conformational Transformation in Thermo-Sensitive and Non-Thermo-Sensitive Oligomers. *Polymer* **54**, 210 (2013).

[33] M. D. Ben, M. Schoenherr, J. Hutter, and J. VandeVondele, Bulk Liquid Water at Ambient Temperature and Pressure from MP2 Theory. *J. Phys. Chem. Lett.* **4**, 3753 (2013).

[34] T. A. Pascal, D. Scharf, Y. Jung, and T. D. Kühne, On the Absolute Thermodynamics of Water from Computer Simulations: A Comparison of First-Principles Molecular Dynamics, Reactive and Empirical Force Fields. *J. Chem. Phys.* **137**, 244507 (2012).

[35] V. Babin, G. R. Medders, and F. Paesani, Toward a Universal Water Model: First Principles Simulations from the Dimer to the Liquid Phase. *J. Phys. Chem. Lett.* **3**, 3765 (2012).

[36] R. Iftimie, P. Minary, and M. E. Tuckerman, Ab Initio Molecular Dynamics: Concepts, Recent Developments, and Future Trends. *Proc. Nat. Acad. Sci. U.S.A.* **102**, 6654 (2005).

[37] J. VandeVondele, F. Mohamed, M. Krack, J. Hutter, M. Sprik, and M. Parrinello, The Influence of Temperature and Density Functional Models in Ab Initio Molecular Dynamics Simulation of Liquid Water. *J. Chem. Phys.* **112**, 014515 (2005).

[38] I.-C. Lin, A. P. Seitsonen, I. Tavernelli, and U. Rothlisberger, Structure and Dynamics of Liquid Water from Ab Initio Molecular Dynamics - Comparison of BLYP, PBE, and revPBE Density Functionals with and without van der Waals Corrections. *J. Chem. Theory Comput.* **8**, 3902 (2012).

[39] Y. Tu and A. Laaksonen, Implementing Quantum Mechanics into Molecular Mechanics - Combined QM/MM Modeling Methods. *Adv. Quantum Chem.* **59**, 1 (2010).

[40] T. S. Hofer, A. B. Pribil, B. R. Randolf, and B. M. Rode, Ab Initio Quantum Mechanical Charge Field Molecular Dynamics-A Nonparametrized First-Principle Approach to Liquids and Solutions. *Adv. Quantum Chem.* **59**, 213 (2010).

[41] N. Bernstein, C. Varnai, I. Solt, S. A. Winfield, M. C. Payne, I. Simon, M. Fuxreiter, and G. Csanyi, QM/MM Simulation of Liquid Water with an Adaptive Quantum Region. *Phys. Chem. Chem. Phys.* **14**, 646 (2012).

[42] F. Paesani and G. A. Voth, The Properties of Water: Insights from Quantum Simulations. *J. Phys. Chem. B* **113**, 5702 (2009).

[43] K. R. Wilson, J. G. Tobin, A. L. Ankudinov, J. J. Rehr, and R. J. Saykally, Extended X-Ray Absorption Fine Structure from Hydrogen Atoms in Water. *Phys. Rev. Lett.* **85**, 4289 (2000).

[44] K. R. Wilson, B. S. Rude, T. Catalano, R. D. Schaller, J. G. Tobin, D. T. Co, and R. J. Saykally, X-ray Spectroscopy of Liquid Water Microjets. *J. Phys. Chem. B* **105**, 3346 (2001).

[45] K. M. Lange, M. Soldatov, R. Golnak, M. Gotz, N. Engel, R. Könnecke, J.-E. Rubensson, and E. F. Aziz, X-ray Emission from Pure and Dilute H_2O and D_2O in a Liquid Microjet: Hydrogen Bonds and Nuclear Dynamics. *Phys. Rev. B* **85**, 155104 (2012).

[46] M. Odelius, Information Content in O[1s] K-edge X-ray Emission Spectroscopy of Liquid Water. *J. Phys. Chem. A* **113**, 8176 (2009).

[47] T. Tokushima, Y. Harada, Y. Horikawa, O. Takahashi, Y. Senba, H. Ohashi, L. G. M. Pettersson, A. Nilsson, and S. Shin, High Resolution X-ray Emission Spectroscopy of Water and Its Assignment Based on Two Structural Motifs. *J. Electron Spectrosc. Relat. Phenom.* **177**, 192 (2010).

[48] O. Fuchs, M. Zharnikov, L. Weinhardt, M. Blum, M. Weigand, Y. Zubavichus, M. Bär, F. Maier, J. D. Denlinger, C. Heske, M. Grunze, and E. Umbach, Isotope and Temperature Effects in Liquid Water Probed by X-Ray Absorption and Resonant X-Ray Emission Spectroscopy. *Phys. Rev. Lett.* **100**, 027801 (2008).

[49] T. Tokushima, Y. Harada, O. Takahashi, Y. Senba, H. Ohashi, L. G. M. Pettersson, A. Nilsson, and S. Shin, High Resolution X-ray Emission Spectroscopy of Liquid Water: The Observation of Two Structural Motifs. *Chem. Phys. Lett.* **460**, 387 (2008).

[50] J.-H. Guo, Y. Luo, A. Augustsson, J.-E. Rubensson, C. Såthe, H. Ågren, H. Siegbahn, and J. Nordgren, X-Ray Emission Spectroscopy of Hydrogen Bonding and Electronic Structure of Liquid Water. *Phys. Rev. Lett.* **89**, 137402 (2002).

[51] A. Nilsson, T. Tokushima, Y. Horikawa, Y. Harada, M. P. Ljungberg, S. Shin, and L. G. M. Pettersson, Resonant Inelastic X-ray Scattering of Liquid Water. *J. Electron Spectrosc. Relat. Phenom.* **188**, 84 (2013).

[52] Y. Harada, T. Tokushima, Y. Horikawa, O. Takahashi, H. Niwa, M. Kobayashi, M. Oshima, Y. Senba, H. Ohashi, K. T. Wikfeldt, A. Nilsson, L. G. M. Pettersson, and S. Shin, Selective Probing of the OH or OD Stretch Vibration in Liquid Water Using Resonant Inelastic Soft-X-Ray Scattering. *Phys. Rev. Lett.* **111**, 193001 (2013).

[53] J. Forsberg, J. Gråsjö, B. Brena, J. Nordgren, L.-C. Duda, and J.-E. Rubensson, Angular Anisotropy of Resonant Inelastic Soft X-ray Scattering from Liquid Water. *Phys. Rev. B* **79**, 132203 (2009).

[54] A. Nilsson, D. Nordlund, I. Waluyo, N. Huang, H. Ogasawara, S. Kaya, U. Bergmann, L.-Å. Näslund, H. Öström, P. Wernet, K. Andersson, T. Schiros, and L. Pettersson, X-ray Absorption Spectroscopy and X-ray Raman Scattering of Water and Ice; an Experimental View. *J. Electron Spectrosc. Relat. Phenom.* **177**, 99 (2010).

[55] C. J. Sahle, C. Sternemann, C. Schmidt, S. Lehtola, S. Jahn, L. Simonelli, S. Huotari, M. Hakala, T. Pylkkänen, A. Nyrow, K. Mende, M. Tolan, K. Hämäläinen, and M. Wilke, Microscopic Structure of Water at Elevated Pressures and Temperatures. *Proc. Nat. Acad. Sci. U.S.A.* **110**, 6301 (2013).

[56] T. Pylkkänen, A. Sakko, M. Hakala, K. Hämäläinen, G. Monaco, and S. Huotari, Temperature Dependence of the Near-Edge Spectrum of Water. *J. Phys. Chem. B* **115**, 14544 (2011).

[57] P. Wernet, D. Nordlund, U. Bergmann, M. Cavalleri, M. Odelius, H. Ogasawara, L. Å. Näslund, T. K. Hirsch, L. Ojamäe, P. Glatzel, L. G. M. Pettersson, and A. Nilsson, The Structure of the First Coordination Shell in Liquid Water. *Science* **304**, 995 (2004).

[58] J. D. Smith, C. D. Cappa, K. R. Wilson, B. M. Messer, R. C. Cohen, and R. J. Saykally, Energetics of Hydrogen Bond Network Rearrangements in Liquid Water. *Science* **306**, 851 (2004).

[59] J. D. Smith, C. D. Cappa, B. M. Messer, W. S. Drisdell, R. C. Cohen, and R. J. Saykally, Probing the Local Structure of Liquid Water by X-ray Absorption Spectroscopy. *J. Phys. Chem. B* **110**, 20038 (2006).

[60] U. Bergmann, P. Wernet, P. Glatzel, M. Cavalleri, L. G. M. Pettersson, A. Nilsson, and S. P. Cramer, X-ray Raman Spectroscopy at the Oxygen K Edge of Water and Ice: Implications on Local Structure Models. *Phys. Rev. B* **66**, 092107 (2002).

[61] S. Myneni, Y. Luo, L. Å. Näslund, M. Cavalleri, L. Ojamäe, H. Ogasawara, A. Pelmenschikov, P. Wernet, P. Väterlein, C. Heske, Z. Hussain, L. G. M. Pettersson, and A. Nilsson, Spectroscopic Probing of Local Hydrogen-Bonding Structures in Liquid Water. *J. Phys.: Condens. Matter* **14**, L213 (2002).

[62] J. S. Tse, D. M. Shaw, D. D. Klug, S. Patchkovskii, G. Vankó, G. Monaco, and M. Krisch, X-ray Raman Spectroscopic Study of Water in the Condensed Phases. *Phys. Rev. Lett.* **100**, 095502 (2008).

[63] T. Pylkkänen, V. M. Giordano, J.-C. Chervin, A. Sakko, M. Hakala, J. A. Soininen, K. Hämäläinen, G. Monaco, and S. Huotari, Role of Non-Hydrogen-Bonded Molecules in the Oxygen K-Edge Spectrum of Ice. *J. Phys. Chem. B* **114**, 3804 (2010).

[64] P. Parent, C. Laffon, C. Mangeney, F. Bournel, and M. Tronc, Structure of the Water Ice Surface Studied by X-ray Absorption Spectroscopy at the O K-edge. *J. Chem. Phys.* **117**, 10842 (2002).

[65] T. T. Fister, K. P. Nagle, F. D. Vila, G. T. Seidler, C. Hammer, J. O. Cross, and J. J. Rehr, Intermediate-Range Order in Water Ices: Nonresonant Inelastic X-ray Scattering Measurements and Real-Space Full Multiple Scattering Calculations. *Phys. Rev. B* **79**, 174117 (2009).

[66] Y. Q. Cai, H.-K. Mao, P. C. Chow, J. S. Tse, Y. Ma, S. Patchkovskii, J. F. Shu, V. Struzhkin, R. J. Hemley, H. Ishii, C. C. Chen, I. Jarrige, C. T. Chen, S. R. Shieh, E. P. Huang, and C. C. Kao, Ordering of Hydrogen Bonds in High-Pressure Low-Temperature H_2O. *Phys. Rev. Lett.* **94**, 025502 (2005).

[67] N. Huang, D. Nordlund, C. Huang, U. Bergmann, T. M. Weiss, L. G. M. Pettersson, and A. Nilsson, X-ray Raman Scattering Provides Evidence for Interfacial Acetonitrile-Water Dipole Interactions in Aqueous Solutions. *J. Chem. Phys.* **135**, 164509 (2011).

[68] M. Cavalleri, L.-Å. Näslund, D. C. Edwards, P. Wernet, H. Ogasawara, S. Myneni, L. Ojamäe, M. Odelius, A. Nilsson, and L. G. M. Pettersson, The Local Structure of Protonated Water from X-ray Absorption and Density Functional Theory. *J. Chem. Phys.* **124**, 194508 (2006).

[69] L.-Å. Näslund, D. C. Edwards, P. Wernet, U. Bergmann, H. Ogasawara, L. G. M. Pettersson, S. Myneni, and A. Nilsson, X-ray Absorption Spectroscopy Study of the Hydrogen Bond Network in the Bulk Water of Aqueous Solutions. *J. Phys. Chem. A* **109**, 5995 (2005).

[70] E. D. Isaacs, A. Shukla, P. M. Platzman, D. R. Hamann, B. Barbiellini, and C. A. Tulk, Covalency of the Hydrogen Bond in Ice: A Direct X-Ray Measurement. *Phys. Rev. Lett.* **82**, 600 (1999).

[71] E. D. Isaacs, A. Shukla, P. M. Platzman, D. R. Hamann, B. Barbiellini, and C. A. Tulk, Compton Scattering Evidence for Covalency of the Hydrogen Bond in Ice. *J. Phys. Chem. Solids* **61**, 403 (2000).

[72] T. K. Ghanty, V. N. Staroverov, P. R. Koren, and E. R. Davidson, Is the Hydrogen Bond in Water Dimer and Ice Covalent? *J. Am. Chem. Soc.* **122**, 1210 (2000).

[73] P. H.-L. Sit, C. Bellin, B. Barbiellini, D. Testemale, J.-L. Hazemann, T. Buslaps, N. Marzari, and A. Shukla, Hydrogen Bonding and Coordination in Normal and Supercritical Water from X-ray Inelastic Scattering. *Phys. Rev. B* **76**, 245413 (2007).

[74] K. Nygård, M. Hakala, S. Manninen, M. Itou, Y. Sakurai, and K. Hämäläinen, Configurational Energetics in Ice Ih Probed by Compton Scattering. *Phys. Rev. Lett.* **99**, 197401 (2007).

[75] K. Nygård, M. Hakala, T. Pylkkänen, S. Manninen, T. Buslaps, M. Itou, A. Andrejczuk, Y. Sakurai, M. Odelius, and K. Hämäläinen, Isotope Quantum Effects in the Electron Momentum Density of Water. *J. Chem. Phys.* **126**, 154508 (2007).

[76] K. Nygård, M. Hakala, S. Manninen, A. Andrejczuk, M. Itou, Y. Sakurai, L. G. M. Pettersson, and K. Hämäläinen, Compton Scattering Study of Water Versus Ice Ih: Intra- and Intermolecular Structure. *Phys. Rev. E* **74**, 031503 (2006).

[77] M. Hakala, K. Nygård, S. Manninen, S. Huotari, T. Buslaps, A. Nilsson, L. G. M. Pettersson, and K. Hämäläinen, Correlation of Hydrogen Bond Lengths and Angles in Liquid Water Based on Compton Scattering. *J. Chem. Phys.* **125**, 084504 (2006).

[78] S. Ragot, J.-M. Gillet, and P. J. Becker, Interpreting Compton Anisotropy of Ice I_h: A Cluster Partitioning Method. *Phys. Rev. B* **65**, 235115 (2002).

[79] C. Bellin, B. Barbiellini, S. Klotz, T. Buslaps, G. Rousse, T. Strässle, and A. Shukla, Oxygen Disorder in Ice Probed by X-ray Compton Scattering. *Phys. Rev. B* **83**, 094117 (2011).

[80] D. F. Reiter, A. Deb, Y. Sakurai, M. Itou, V. G. Krishnan, and S. J. Paddison, Anomalous Ground State of the Electrons in Nanoconfined Water. *Phys. Rev. Lett.* **111**, 036803 (2013).

[81] K. Nygård, M. Hakala, S. Manninen, K. Hämäläinen, M. Itou, A. Andrejczuk, and Y. Sakurai, Ion Hydration Studied by X-ray Compton Scattering. *Phys. Rev. B* **73**, 024208 (2006).

[82] M. Hakala, S. Huotari, K. Hämäläinen, S. Manninen, P. Wernet, A. Nilsson, and L. G. M. Pettersson, Compton Profiles for Water and Mixed Water-Neon Clusters: A Measure of Coordination. *Phys. Rev. B* **70**, 125413 (2004).

[83] M. Hakala, K. Nygård, J. Vaara, M. Itou, Y. Sakurai, and K. Hämäläinen, Charge Localization in Alcohol Isomers Studied by Compton Scattering. *J. Chem. Phys.* **130**, 034506 (2009).

[84] F. Lehmkühler, A. Sakko, I. Steinke, C. Sternemaan, M. Hakala, C. J. Sahle, T. Buslaps, L. Simonelli, S. Galambosi, M. Paulus, T. Pylkkänen, M. Tolan, and K. Hämäläinen, Temperature-Induced Structural Changes of Tetrahydrofuran Clathrate and of the Liquid Water/Tetrahydrofuran Mixture. *J. Phys. Chem. C* **115**, 21009 (2011).

[85] F. Lehmkühler, A. Sakko, C. Sternemann, M. Hakala, K. Nygård, C. J. Sahle, S. Galambosi, I. Steinke, S. Tiemeyer, A. Nyrow, T. Buslaps, D. Pontoni, M. Tolan, and K. Hämäläinen, Anomalous Energetics in Tetrahydrofuran Clathrate Hydrate Revealed by X-ray Compton Scattering. *J. Phys. Chem. Lett.* **1**, 2832 (2010).

[86] C. Sternemann, S. Huotari, M. Hakala, M. Paulus, M. Volmer, C. Gutt, T. Buslaps, N. Hiraoka, D. D. Klug, K. Hämäläinen, M. Tolan, and J. S. Tse, Electronic Structure of Methane Hydrate Studied by Compton Scattering. *Phys. Rev. B* **73**, 195104 (2006).

[87] E. Arunan, G. R. Desiraju, R. A. Klein, J. Sadlej, S. Scheiner, I. Alkorta, D. C. Clary, R. H. Crabtree, J. J. Dannenberg, P. Hobza, H. G. Kjaergaard, A. C. Legon, B. Mennucci, and D. J. Nesbitt, Definition of the hydrogen bond (IUPAC Recommendations 2011). *Pure Appl. Chem.* **83**, 1637 (2011).

[88] A. D. Buckingham, J. E. D. Bene, and S. A. C. McDowell, The Hydrogen Bond. *Chem. Phys. Lett.* **463**, 1 (2008).

[89] E. Ramos-Cordoba, D. S. Lambrecht, and M. Head-Gordon, Charge-Transfer and the Hydrogen Bond: Spectroscopic and Structural Implications from Electronic Structure Calculations. *Faraday Discuss.* **150**, 345 (2011).

[90] F. H. Stillinger, Water Revisited. *Science* **209**, 451 (1980).

[91] N. J. English, P. G. Kusalik, and J. S. Tse, Density Equalisation in Supercooled High- and Low-Density Water Mixtures. *J. Chem. Phys.* **139**, 084508 (2013).

[92] H. J. Bakker, S. Woutersen, and H.-K. Nienhuys, Reorientational Motion and Hydrogen-Bond Stretching Dynamics in Liquid Water. *Chem. Phys.* **258**, 233 (2000).

[93] C. J. Fecko, J. J. Loparo, S. T. Roberts, and A. Tokmakoff, Local Hydrogen Bonding Dynamics and Collective Reorganization in Water: Ultrafast Infrared Spectroscopy of HOD/D_2O. *J. Chem. Phys.* **122**, 054506 (2005).

[94] T. Steinel, J. B. Asbury, J. Zheng, and M. D. Fayer, Watching Hydrogen Bonds Break: A Transient Absorption Study of Water. *J. Phys. Chem. A* **108**, 10957 (2004).

[95] J. D. Eaves, J. J. Loparo, C. J. Fecko, S. T. Roberts, A. Tokmakoff, and P. L. Geissler, Hydrogen Bonds in Liquid Water are Broken Only Fleetingly. *Proc. Nat. Acad. Sci. U.S.A.* **102**, 13019 (2005).

[96] M. Candotti, S. Esteban-Martin, X. Salvatella, and M. Orozco, Toward an Atomistic Description of the Urea-Denatured State of Proteins. *Proc. Nat. Acad. Sci. U.S.A.* **110**, 5933 (2013).

[97] Y. Hayashi, Y. Katsumoto, S. Omori, N. Kishii, and A. Yasuda, Liquid Structure of the Urea-Water System Studied by Dielectric Spectroscopy. *J. Phys. Chem. B* **111**, 1076 (2007).

[98] S. Funkner, M. Havenith, and G. Schwaab, Urea, a Structure Breaker? Answers from THz Absorption Spectroscopy. *J. Phys. Chem. B* **116**, 13374 (2012).

[99] A. K. Soper, E. W. Castner, and A. Luzar, Impact of Urea on Water Structure: a Clue to Its Properties as a Denaturant? *Biophys. Chem.* **105**, 649 (2003).

[100] J. K. Carr, L. E. Buchanan, J. R. Schmidt, M. T. Zanni, and J. L. Skinner, Structure and Dynamics of Urea/Water Mixtures Investigated by Vibrational Spectroscopy and Molecular Dynamics Simulation. *J. Phys. Chem. B* **117**, 13291 (2013).

[101] Y. L. A. Rezus and H. J. Bakker, Effect of Urea on the Structural Dynamics of Water. *Proc. Nat. Acad. Sci. U.S.A.* **103**, 18417 (2006).

[102] H. Wei, Y. Fan, and Y. Gao, Effects of Urea, Tetramethyl Urea, and Trimethylamine N-Oxide on Aqueous Solution Structure and Solvation of Protein Backbones: A Molecular Dynamics Simulation Study. *J. Phys. Chem. B* **133**, 557 (2010).

[103] B. Bennion and V. Daggett, The Molecular Basis for the Chemical Denaturation of Proteins by Urea. *Proc. Nat. Acad. Sci. U.S.A.* **100**, 5142 (2003).

[104] A. Idrissi, M. Gerard, P. Damay, M. Kiselev, Y. Puhovsky, E. Cinar, P. Lagant, and G. Vergoten, The Effect of Urea on the Structure of Water: A Molecular Dynamics Simulation. *J. Phys. Chem. B* **114**, 4731 (2010).

[105] R. Chitra and P. E. Smith, Molecular Association in Solution: A Kirkwood-Buff Analysis of Sodium Chloride, Ammonium Sulfate, Guanidium Chloride, Urea, and 2,2,2-Trifluoroethanol in Water. *J. Phys. Chem. B* **106**, 1491 (2002).

[106] M. C. Stumpe and H. Grubmüller, Aqueous Urea Solutions: Structure, Energetics, and Urea Aggregation. *J. Phys. Chem. B* **114**, 6220 (2007).

[107] F. Hofmeister, Zur Lehre von der Wirkung der Salze. *Arch. Exp. Pathol. Pharmakol.* **24**, 247 (1888).

[108] K. D. Collins and M. W. Washabaugh, The Hofmeister Effect and the Behavior of Water at Interfaces. *Q. Rev. Biophys.* **18**, 323 (1985).

[109] M. Yizhak, Effect of Ions on the Structure of Water: Structure Making and Breaking. *Chem. Rev.* **109**, 1346 (2009).

[110] A. W. Omta, M. F. Kropman, S. Woutersen, and H. J. Bakker, Negligible Effect of Ions on the Hydrogen-Bond Structure in Liquid Water. *Science* **301**, 347 (2003).

[111] C. D. Cappa, J. D. Smith, B. M. Messer, R. C. Cohen, and R. J. Saykally, Effects of Cations on the Hydrogen Bond Network of Liquid Water: New Results from X-ray Absorption Spectroscopy of Liquid Microjets. *J. Phys. Chem. B* **110**, 5301 (2006).

[112] K. D. Collins, G. W. Neilson, and J. E. Enderby, Ions in Water: Characterizing the Forces That Control Chemical Processes and Biological Structure. *Biophys. Chem.* **128**, 95 (2007).

[113] P. Gallo, D. Corradini, and M. Rovere, Ion Hydration and Structural Properties of Water in Aqueous Solutions at Normal and Supercooled Conditions: a Test of the Structure Making and Breaking Concept. *Phys. Chem. Chem. Phys.* **13**, 19814 (2011).

[114] R. Mancinelli, A. Botti, F. Bruni, M. A. Ricci, and A. K. Soper, Hydration of Sodium, Potassium, and Chloride Ions in Solution and the Concept of Structure Maker/Breaker. *J. Phys. Chem. B* **111**, 13570 (2007).

[115] T. Corridoni, R. Mancinelli, M. A. Ricci, and F. Bruni, Viscosity of Aqueous Solutions and Local Microscopic Structure. *J. Phys. Chem. B* **115**, 14008 (2011).

[116] L. Stryer and R. P. Haugland, Energy Transfer - a Spectroscopic Ruler. *Proc. Nat. Acad. Sci. U.S.A.* **58**, 719 (1967).

[117] J. L. Fulton and M. Balasubramanian, Structure of Hydronium H_3O^+/Chloride (Cl^-) Contact Ion Pairs in Aqueous Hydrochloric Acid Solution: A Zundel-Like Local Configuration. *J. Am. Chem. Soc.* **132**, 12597 (2010).

[118] H. J. Kulik, N. Marzari, A. A. Correa, D. Prendergast, E. Schwegler, and G. Galli, Local Effects in the X-ray Absorption Spectrum of Salt Water. *J. Phys. Chem. B* **114**, 9594 (2010).

[119] R. Mancinelli, A. Botti, F. Bruni, M. A. Ricci, and A. K. Soper, Perturbation of Water Structure Due to Monovalent Ions in Solution. *Phys. Chem. Chem. Phys.* **9**, 2959 (2007).

[120] A. K. Soper and K. Weckström, Ion Solvation and Water Structure in Potassium Halide Aqueous Solutions. *Biophys. Chem.* **124**, 180 (2006).

[121] L. Petit, R. Vuilleumier, P. Maldivi, and C. Adamo, Ab Initio Molecular Dynamics Study of a Highly Concentrated LiCl Aqueous Solution. *J. Chem. Theory Comput.* **4**, 1040 (2008).

[122] T. Yamaguchi, H. Ohzono, M. Yamagami, K. Yamanaka, K. Yoshida, and H. Wakita, Ion Hydration in Aqueous Solutions of Lithium Chloride, Nickel Chloride, and Caesium Chloride in Ambient to Supercritical Water. *J. Mol. Liq.* **153**, 2 (2010).

[123] S. B. Rempe, L. R. Pratt, G. Hummer, J. D. Kress, R. L. Martin, and A. Redondo, The Hydration Number of Li^+ in Liquid Water. *J. Am. Chem. Soc.* **122**, 966 (2000).

[124] S. Varma and S. B. Rempe, Coordination Numbers of Alkali Metal Ions in Aqueous Solutions. *Biophys. Chem.* **124**, 192 (2006).

[125] I. Harsányi and L. Pusztai, On the Structure of Aqueous LiCl Solutions. *J. Chem. Phys.* **122**, 124512 (2005).

[126] D. Spångberg, R. Rey, J. T. Hynes, and K. Hermansson, Rate and Mechanism for Water Exchange around Li^+(aq) from MD Simulations. *J. Phys. Chem. B* **107**, 4470 (2003).

[127] T. Cartailler, W. Kunz, P. Turq, and M.-C. Bellisent-Funel, Lithium Bromide in Acetonitrile and Water - a Neutron-Scattering Study. *J. Phys.: Condens. Matter* **3**, 9511 (1991).

[128] A. Musinu, G. Paschina, G. Piccaluga, and M. Magini, X-ray-Diffraction Study of $CoCl_2$-LiCl Aqueous Solutions. *J. Chem. Phys.* **80**, 2772 (1984).

[129] I. Harsányi, P. A. Bopp, A. Vrhovšek, and L. Pusztai, On the Hydration Structure of LiCl Aqueous Solutions: A Reverse Monte Carlo Based Combination of Diffraction Data and Molecular Dynamics Simulations. *J. Mol. Liq.* **158**, 61 (2011).

[130] J. R. Newsome, G. W. Neilson, and J. E. Enderby, Lithium Ions in Aqueous Solutions. *J. Phys. C.: Solid State Phys.* **13**, L923 (1980).

[131] I. Howell and G. W. Neilson, Li+ Hydration in Concentrated Aqueous Solution. *J. Phys.: Condens. Matter* **8**, 4455 (1996).

[132] H. S. Frank and M. W. Evans, Free Volume and Entropy in Condensed Systems III. Entropy in Binary Liquid Mixtures; Partial Molal Entropy in Dilute Solutions; Structure and Thermodynamics in Aqueous Electrolytes. *J. Chem. Phys.* **13**, 507 (1945).

[133] A. D. Sloan and C. A. Koh, editors, Clathrate Hydrates of Natural Gases, Third Edition. CRC Press, Boca Raton (2008).

[134] J. G. Davis, K. P. Gierszal, P. Wang, and D. Ben-Amotz, Water Structural Transformation at Molecular Hydrophobic Interfaces. *Nature* **491**, 582 (2012).

[135] N. Galamba, Water's Structure around Hydrophobic Solutes and the Iceberg Model. *J. Phys. Chem. B* **117**, 2153 (2013).

[136] T. M. Raschke and M. Levitt, Nonpolar Solutes Enchance Water Structure Within Hydration Shells while Reducing Interactions Between Them. *Proc. Nat. Acad. Sci. U.S.A.* **102**, 6777 (2005).

[137] J. Qvist and B. Halle, Thermal Signature of Hydrophobic Hydration Dynamics. *J. Am. Chem. Soc.* **130**, 10345 (2008).

[138] J. Tomlinson-Phillips, J. Davis, D. Ben-Amotz, D. Spångberg, L. Pejov, and K. Hermansson, Structure and Dynamics of Water Dangling OH Bonds in Hydrophobic Hydration Shells. Comparison of Simulation and Experiment. *J. Phys. Chem. A* **115**, 6177 (2011).

[139] P. Buchanan, N. Aldiwan, A. K. Soper, J. L. Creek, and C. A. Koh, Decreased Structure on Dissolving Methane in Water. *Chem. Phys. Lett.* **415**, 89 (2005).

[140] S. Garde and A. J. Patel, Unraveling the Hydrophobic Effect, One Molecule at a Time. *Proc. Nat. Acad. Sci. U.S.A.* **108**, 16491 (2011).

[141] J. T. King, E. J. Arthur, C. L. Brooks, and K. J. Kubarych, Site-Specific Hydration Dynamics of Globular Proteins and the Role of Constrained Water in Solvent Exchange with Amphiphilic Cosolvents. *J. Phys. Chem. B* **116**, 5604 (2012).

[142] D. Chandler, Interfaces and the Driving Force of Hydrophobic Assembly. *Nature* **437**, 640 (2005).

[143] W. Schülke, Electron Dynamics by Inelastic X-Ray Scattering. Oxford University Press (2007).

[144] S. Lehtola, ERKALE - HF/DFT from Hel (2012).

[145] J. Lehtola, M. Hakala, A. Sakko, and K. Hämäläinen, ERKALE - A Flexible Program Package for X-ray Properties of Atoms and Molecules. *J. Chem. Phys.* **33**, 1572 (2012).

[146] C. Sternemann, M. Volmer, J. A. Soininen, H. Nagasawa, M. Paulus, H. Enkisch, G. Schmidt, M. Tolan, and W. Schülke, Momentum-Transfer Dependence of X-ray Raman Scattering at the Be K-edge. *Phys. Rev. B* **68**, 035111 (2003).

[147] C. J. Sahle, C. Sternemaan, H. Sternemann, J. S. Tse, R. A. Gordon, S. Desgreniers, S. Maekawa, S. Yamanaka, F. Lehmkühler, D. C. F. Wieland, K. Mende, S. Huotari, and M. Tolan, The Ba 4d-4f Giant Dipole Resonance in Complex Ba/Si Compounds. *J. Phys. B: At. Mol. Opt. Phys.* **47**, 045102 (2014).

[148] R. A. Gordon, G. T. Seidler, T. T. Fister, M. W. Havenkort, G. A. Sawatzky, A. Tanaka, and T. K. Sham, High Multipole Transitions in NIXS: Valence and Hybridization in 4f Systems. *Europhys. Lett.* **81**, 26004 (2008).

[149] K. P. Nagle, G. T. Seidler, E. L. Shirley, T. T. Fister, J. A. Bradley, and F. C. Brown, Final-State Symmetry of Na 1s Core-Shell Excitons in NaCl and NaF. *Phys. Rev. B* **80**, 045105 (2009).

[150] L. V. Hove, Correlations in Space and Time and Born Approximation Scattering in Systems of Interacting Particles. *Phys. Rev.* **95**, 249 (1954).

[151] P. Eisenberger and P. M. Platzman, Compton Scattering of X-rays from Bound Electrons. *Phys. Rev. A* **2**, 415 (1970).

[152] R. Ribberfors, Relationship of the Relativistic Compton Cross Section to the Momentum Distribution of Bound Electron States. *Phys. Rev. B* **12**, 2067 (1975).

[153] P. Holm, Relativistic Compton Cross Section for General Central-Field Hartree-Fock Wave Functions. *Phys. Rev. A* **37**, 3706 (1988).

[154] Y. Sakurai, High-Energy Inelastic-Scattering Beamline for Electron Momentum Density Study. *J. Synchrotron Rad.* **5**, 208 (1998).

[155] R. Verbeni, T. Pylkkänen, S. Huotari, L. Simonelli, G. Vankó, K. Martel, C. Henriquet, and G. Monaco, Multiple-Element Spectrometer for Non-Resonant Inelastic X-ray Spectroscopy of Electronic Excitations. *J. Synchrotron Rad.* **16**, 469 (2009).

[156] S. Huotari, T. Pylkkänen, R. Verdeni, G. Monaco, and K. Hämäläinen, Direct Tomography with Chemical-Bond Contrast. *Nature Mat.* **10**, 489 (2011).

[157] P. Suortti, T. Buslaps, P. Fajardo, V. Honkimäki, M. Kretzschmer, U. Lienert, J. E. McCarthy, M. Renier, A. Shukla, T. Tschentscher, and T. Meinander, Scanning X-ray Spectrometer for High-Resolution Compton Profile Measurements at ESRF. *J. Synchrotron Rad.* **6**, 69 (1999).

[158] C. Laffon, S. Lacombe, F. Bournel, and P. Parent, Radiation Effects in Water Ice: A Near-Edge X-ray Absorption Fine Structure Study. *J. Chem. Phys.* **125**, 204714 (2006).

[159] W. L. Mao, H.-K. Mao, Y. Meng, P. J. Eng, M. Y. Hu, P. Chow, Y. Q. Cai, J. Shu, and R. J. Hemley, X-ray-Induced Dissociation of H_2O and Formation of an O_2-H_2 Alloy at High Pressure. *Science* **314**, 636 (2006).

[160] M. Born and R. Oppenheimer, Zur Quantentheorie der Molekeln. *Ann. Phys.* **389**, 457 (1927).

[161] K. Burke and L. O. Wagner, DFT in a Nutshell. *Int. J. Quantum Chem.* **113**, 96 (2013).

[162] R. G. Parr and W. Yang, Density-Functional Theory of Atoms and Molecules. Oxford University Press (1989).

[163] W. Kohn and L. J. Sham, Inhomogeneous Electron Gas. *Phys. Rev.* **140**, A1133 (1965).

[164] J. P. Perdew, K. Burke, and M. Ernzerhof, Generalized Gradient Approximation Made Simple. *Phys. Rev. Lett.* **77**, 3865 (1996).

[165] J. P. Perdew, K. Burke, and M. Ernzerhof, Generalized Gradient Approximation Made Simple [Phys. Rev. Lett. 77, 3865 (1996)]. *Phys. Rev. Lett.* **78**, 1396 (1997).

[166] K. Burke, M. Ernzerhof, and J. P. Perdew, The Adiabatic Connection Method: A Non-Empirical Hybrid. *Chem. Phys. Lett.* **265**, 115 (1997).

[167] A. D. Becke, Density-Functional Exchange-Energy Approximation with Correct Asymptotic Behavior. *Phys. Rev. A* **38**, 3098 (1988).

[168] C. Lee, W. Yang, and R. G. Parr, Development of the Colle-Salvetti Correlation-Energy Formula into a Functional of the Electron Density. *Phys. Rev. B* **37**, 785 (1988).

[169] A. D. Becke, Density-Functional Thermochemistry .3. The Role of Exact Exchange. *J. Chem. Phys.* **98**, 5648 (1993).

[170] R. Stowasser and R. Hoffmann, What Do the Kohn-Sham Orbitals and Eigenvalues Mean? *J. Am. Chem. Soc.* **121**, 3414 (1999).

[171] A. Savin, C. J. Umrigar, and X. Gonze, Relationship of Kohn-Sham Eigenvalues to Excitation Energies. *Chem. Phys. Lett.* **288**, 391 (1998).

[172] I. R. Epstein and W. N. Lipscomb, Molecular Momentum Distributions and Compton Profiles. I. General Theory and Boron Hydrides. *J. Chem. Phys.* **53**, 4418 (1970).

[173] K. Hermann, L. Pettersson, M. Casida, C. Daul, A. Goursot, A. Koester, E. Proynov, A. St-Amant, and D. Salahub, StoBe-deMon version 3.1 (2011).

[174] L. Triguero, L. G. M. Pettersson, and H. Ågren, Calculations of Near-Edge X-ray-Absorption Spectra of Gas-Phase and Chemisorbed Molecules by Means of Density-Functional and Transition-Potential Theory. *Phys. Rev. B* **58**, 8097 (1998).

[175] J. C. Slater and K. H. Johnson, Self-Consistent-Field $X\alpha$ Cluster Method for Polyatomic Molecules and Solids. *Phys. Rev. B* **5**, 844 (1972).

[176] M. Cavalleri, M. Odelius, D. Nordlund, A. Nilsson, and L. G. M. Pettersson, Half or Full Core Hole in Density Functional Theory X-ray Absorption Spectrum Calculations of Water? *Phys. Chem. Chem. Phys.* **7**, 2854 (2005).

[177] M. Leetmaa, M. P. Ljungberg, A. Lyubartsev, A. Nilsson, and L. G. M. Pettersson, Theoretical Approximations to X-ray Absorption Spectroscopy of Liquid Water and Ice. *J. Electron Spectrosc. Relat. Phenom.* **177**, 135 (2010).

[178] H. J. C. Berendsen, D. van der Spoel, and R. van Drunen, Gromacs - a Message-Passing Parallel Molecular-Dynamics Implementation. *Comput. Phys. Commun.* **91**, 43 (1995).

[179] W. L. Jorgensen, D. S. Maxwell, and J. Tirado-Rives, Development and Testing of the OPLS All-Atom Force Field on Conformational Energetics and Properties of Organic Liquids. *J. Am. Chem. Soc.* **118**, 11225 (1996).

[180] W. L. Jorgensen, J. Chandrasekhar, J. D. Madura, R. W. Impey, and M. L. Klein, Comparison of Simple Potential Functions for Simulating Liquid Water. *J. Chem. Phys.* **79**, 926 (1983).

[181] M. J. Cooper, P. E. Mijnarends, N. Shiotani, N. Sakai, and A. Bansil, editors, X-ray Compton Scattering. Oxford University, Oxford (2004).

[182] H. Sternemann, C. Sternemann, G. T. Seidler, T. T. Fister, A. Sakko, and M. Tolan, An Extraction Algorithm for Core-Level Excitations in Non-Resonant Inelastic X-Ray Scattering Spectra. *J. Synchrotron Rad.* **15**, 162 (2008).

[183] W. Chen, X. Wu, and R. Car, X-ray Absorption Signatures of the Molecular Environment in Water and Ice. *Phys. Rev. Lett.* **105**, 017802 (2010).

[184] T. Pylkkänen, J. Lehtola, M. Hakala, A. Sakko, G. Monaco, S. Huotari, and K. Hämäläinen, Universal Signature of Hydrogen Bonding in the Oxygen K-Edge Spectrum of Alcohols. *J. Phys. Chem. B* **114**, 13076 (2010).

[185] S. Kaya, D. Schlesinger, S. Yamamoto, J. T. Newberg, H. Bluhm, H. Ogasawara, T. Kendelewicz, G. E. Brown, L. G. M. Pettersson, and A. Nilsson, Highly Compressed Two-Dimensional Form of Water at Ambient Conditions. *Scientific Reports* **3**, 1074 (2013).

[186] H. Fukui, S. Huotari, D. Andrault, and T. Kawamoto, Oxygen K-edge Fine Structures of Water by X-ray Raman Scattering Spectroscopy under Pressure Conditions. *J. Chem. Phys.* **127**, 134502 (2007).

[187] M. Hakala, K. Nygård, S. Manninen, L. G. M. Pettersson, and K. Hämäläinen, Intra- and Intermolecular Effects in the Compton Profile of Water. *Phys. Rev. B* **73**, 035432 (2006).

[188] K. Winkel, M. Seidl, T. Loerting, L. E. Bove, S. Imberti, V. Molinero, F. Bruni, R. Mancinelli, and M. A. Ricci, Structural Study of Low Concentration LiCl Aqueous Solutions in the Liquid, Supercooled, and Hyperquenched Glassy States. *J. Chem. Phys.* **134**, 024515 (2011).

[189] P. E. Mason, S. Ansell, and G. W. Neilson, Neutron Diffraction Studies of Electrolytes in Null Water: a Direct Determination of the First Hydration Zone of Ions. *J. Phys.: Condens. Matter* **18**, 8437 (2006).

[190] H. J. Kulik, E. Schwegler, and G. Galli, Probing the Structure of Salt Water under Confinement with First-Principles Molecular Dynamics and Theoretical X-ray Absorption Spectroscopy. *J. Phys. Chem. Lett.* **3**, 2653 (2012).

[191] H. Yang, R. Cheng, and Z. Wang, A Quantitative Analyses of the Viscometric Data of the Coil-to-Globule and Globule-to-Coil Transition of Poly(N-isopropylacrylamide) in Water. *Polymer* **44**, 7175 (2003).

[192] S. A. Deshmukh, S. K. R. S. Sankaranarayanan, K. Suthar, and D. C. Mancini, Role of Solvation Dynamics and Local Ordering of Water in Inducing Conformational Transitions in Poly(N-isopropylacrylamide) Oligomers Through the LCST. *J. Phys. Chem. B* **116**, 2651 (2012).

[193] H. Cheng, L. Shen, and C. Wu, LLS and FTIR Studies on the Hysteresis in Association and Dissociation of Poly(N-isopropylacrylamide) Chains in Water. *Macromolecules* **39**, 2325 (2006).

[194] Z. Ahmed, E. A. Gooding, K. V. Pimenov, L. Wang, and S. A. Asher, UV Resonance Raman Determination of Molecular Mechanism of Poly(N-isopropylacrylamide) Volume Phase Transition. *J. Phys. Chem. B* **113**, 4248 (2009).

[195] C. Wu and X. Wang, Globule-to-Coil Transition of a Single Homopolymer Chain in Solution. *Phys. Rev. Lett.* **80**, 4092 (1998).

[196] Y. Lu, K. Zhou, Y. Ding, G. Zhang, and C. Wu, Origin of Hysteresis Observed in Association and Dissociation of Polymer Chains in Water. *Phys. Chem. Chem. Phys.* **12**, 3188 (2010).

[197] K. Zhou, Y. Lu, J. Li, L. Shen, G. Zhang, Z. Xie, and C. Wu, The Coil-to-Globule-to-Coil Transition of Linear Polymer Chains in Dilute Aqueous Solutions: Effect of the Intrachain Hydrogen Bonding. *Macromolecules* **41**, 8927 (2008).

[198] M. R. Berber, H. Mori, I. H. Hafez, K. Minagawa, M. Tanaka, T. Niidome, Y. Katayama, A. Maruyama, T. Hirano, Y. Maeda, and T. Mori, Unusually Large Hysteresis of Temperature-Responsive Poly(N-ethyl-2-propionamidoacrylamide) Studied by Microcalorimetry and FT-IR. *J. Phys. Chem. B* **114**, 7784 (2010).

[199] H. Lai and P. Wu, A Infrared Spectroscopic Study on the Mechanism of Temperature-Induced Phase Transition of Concentrated Aqueous Solutions of Poly(N-isopropylacrylamide) and N-isopropylpropionamide. *Polymer* **51**, 1404 (2010).

[200] G. Longhi, F. Lebon, S. Abbate, and S. L. Fornili, Molecular Dynamics Simulation of a Model Oligomer for Poly(N-isopropylamide) in Water. *Chem. Phys. Lett.* **386**, 123 (2004).

[201] Y. Ono and T. Shikata, Contrary Hydration Behavior of N-Isopropylacrylamide to Its Polymer, P(NIPAm), with a Lower Critical Solution Temperature. *J. Phys. Chem. B* **111**, 1511 (2007).

[202] J. Dybal, M. Trchová, and P. Schmidt, The Role of Water in Structural Changes of Poly(N-isopropylacrylamide) and Poly(N-isopropylmethacrylamide) Studied by FTIR, Raman Spectroscopy and Quantum Chemical Calculations. *Vib. Spectrosc.* **51**, 44 (2009).